history as one of the indicators of product quality, one can, in principle, design appropriate successive processes in a continuous spouted bed dryer to minimize product damage.

Key Words: Dehydration; Diffusion; Non-equilibrium; Paddy; Simulation; Tempering

INTRODUCTION

The combination of two distinct hydrodynamic regimes, pneumatic transport in the spout and a moving bed in the downcomer, is a key feature of the spouted bed. To simulate spouted bed drying, a macroscopic drying model of the overall bed incorporating mass and energy balances and drying rate kinetics is generally developed. Mechanism of drying for the spout and downcomer regions are considered as whole bed. Thermal equilibrium between the grain and the air leaving the bed and well mixed isothermal bed are usually assumed for simplifying model and thus the model does not deal with heat transfer equation (Becker and Sallans (1); Zurith and Singh (2); Zahed and Epstein (3,4); Ngygen (5)). A model for batch drying of rough rice was developed by Zurith and Singh (2) using a semi-theory of the heat desorption-vaporization as a function of temperature and moisture content. To predict the moisture content, Zurith and Singh (2) assumed a constant diffusion coefficient. Unlike Zurith and Singh (2), Zahed and Epstein (3,4) used an empirical equation relating the diffusion coefficient of cereal grains to temperature and moisture content.

Jumah et al. (7,8) developed a model for batch drying of corn in a novel rotating jet spouted bed under conditions of constant and intermittent drying. Unlike prior related works as above-mentioned, the assumptions of thermal equilibrium and of no temperature gradient inside the kernels were not employed in their model. To study drying kinetics of grains in two-dimensional spouted beds, Kalwar and Raghavan (9) dried shelled corn in their experiments under minimum spouting conditions and found that there was no constant drying rate period. However, Wetchacama et al. (11) and Ngugen (5,6) found different results in their study of batch drying of paddy in spouted bed dryers. The results showed that the moisture content reduction with time was nearly constant rate.

Madhiyanon et al. (13) presented the non-equilibrium and non-isothermal bed model for batch drying of grains, which was validated with the experimental results of batch drying of corn in two-dimensional spouted bed dryer (proposed originally by Mujumdar (14)). Unlike the previous studies, modeling of the spout and downcomer regions are

considered separately for better description of the drying physics. The model has to deal with the circulation rate of grains, which has been formulated empirically by Kalwar and Raghavan (10). Clearly, almost of research has been concerned with batch drying, rather than continuous drying of grains in spouted bed dryer. For drying on a commercial scale, continuous operation is always preferable. It is thus the object of this paper to further develop the mathematical model for continuous drying of grains in a spouted bed dryer, with a part of exhausted air recycled.

This model was compared with the experimental results of paddy drying in an industrial-scale continuous spouted bed paddy dryer with a capacity of 2500–3500 kg/h as proposed by Madhiyanon et al. (12). To develop the model, the spouted beds (both the spout and downcomer regions) are divided into elementary thin layers and four differential equations, i.e., mass balance, energy balance, heat transfer and diffusion drying, were developed and solved numerically. Due to low air-to-grain ratios in the downcomer, it may cause much more moisture transfer than ability of the air to carry it. The procedure for checking the limitation of air in the downcomer to adsorb moisture from grains was also incorporated into the model. The model was developed on the assumption of plug flow pattern for grains in a continuous spouted bed dryer. However, for real situations we found that the flow behavior of grains deviated from plug flow. Thus, the model accounts for the deviation of the real system by incorporating an appropriate residence time distribution function into the model; this is similar to the previous works by Becker and Sallons (1), and Zahed and Epstein (3). For an overall review of spouted bed drying techniques, the reader should refer to Pallai et al. (15). For a discussion of the design principles, the reader will find the article by Passos et al. (16) of interest.

MODEL DEVELOPMENT

Assumptions

The following assumptions are made in the development of the mathematical model.

1. The paddy kernels are uniform in size and internally homogeneous, and can be approximated as isotropic spheres.
2. Internal moisture diffusion dominates the drying process, so that the external convective mass transfer resistance can be neglected and the surface moisture content of grains is assumed to reach

3. Moisture migration within the grain kernel is controlled by liquid diffusion.
4. Temperature gradients within the grain kernel are negligible.
5. The effects of heat conduction and moisture transfer between grains, heat losses and grain shrinkage are neglected.
6. The accumulation of the thermal energy and water vapor of the air in the bed is negligible.
7. The airflow and grainflow are in plug flow in both regions, and the co-currentflow and counterflow are assumed for the spout and downcomer regions, respectively.

To simulate drying in the spout and downcomer regions, the bed is assumed to be divided into a series of elementary thin layers (Figure 1) of differential thickness (δy) and unit cross-sectional area. The basic knowledge of mass and energy conservation with accounting for convective heat transfer (air-grain interface) and diffusion mass transfer within the kernel are applied to each elementary thin layer drying, which leads to a set of differential equations. Referring to Mathiyanon et al. (13), the four governing differential equations of mass conservation, energy conservation of air and grain, and diffusional drying kinetics Eqs. (1)–(4) can be rewritten as:

$$G_p \frac{dM}{dy} = \pm G_a \frac{dW}{dy} \tag{1}$$

$$\frac{dT_p}{dy} = \frac{ha_p(T_a - T_p)}{G_p c_p + G_p M c_w} + \frac{\lambda + c_v(T_a - T_p)}{c_p + M c_w} \frac{dM}{dy} \tag{2}$$

$$\frac{dT_a}{dy} = \pm \frac{ha_p(T_a - T_p)}{G_a c_a + G_a W c_v} \tag{3}$$

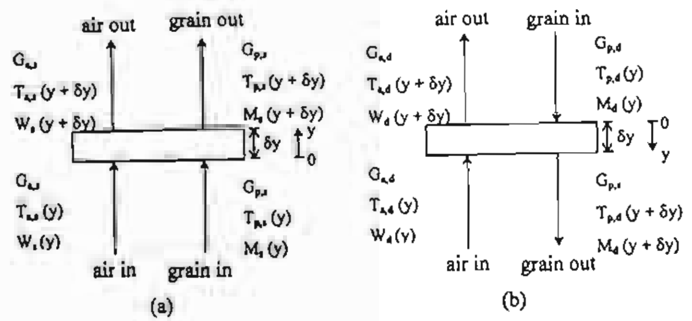

Figure 1. Elementary thin layers. (a) spout region; (b) downcomer region.

Equations (1) and (3) are applied with the minus sign for the spout region with co-currentflow and with the positive sign for the downcomer with counterflow.

To set the boundary conditions for Eqs. (1)–(3), we assume that the outlet conditions of grain for each region are the inlet conditions of the subsequent region and thus we obtain:

For the spout region,

$$
\begin{array}{lll}
y = 0, & t = 0 & T_p = T_{p,in} \quad M = M_{in} \\
 & t > 0 & T_p = T_p \text{ (end of downcomer zone)} \\
 & & M = M \text{ (end of downcomer zone)} \\
y = 0, & t = 0 & T = T_{a,in} \quad W = W_{amb} \\
 & t > 0 & T = T_{a,in} \quad W = W_{mix}
\end{array}
$$

where W_{mix} is the humidity of recirculating air mixed with the ambient air. For the downcomer region,

$$
\begin{array}{lll}
y = 0, & t > 0 & T_p = T_p \text{ (end of spouting zone)} \\
 & & M = M \text{ (end of spouting zone)} \\
y = L, & t = 0 & T_a = T_{a,in} \quad W = W_{amb} \\
 & t > 0 & T_a = T_{a,in} \quad W = W_{mix}
\end{array}
$$

Assuming a constant diffusion coefficient, the equation for one-dimensional diffusion for spherical geometry with appropriate initial and boundary conditions to describe the moisture transfer are:

$$\frac{\partial M}{\partial t} = D\left[\frac{\partial^2 M}{\partial r^2} + \left(\frac{2}{r}\right)\frac{\partial M}{\partial r}\right] \tag{4}$$

$$
\begin{array}{lll}
t = 0, & 0 \le r \le r_p & M = M_{in} \\
t > 0, & r = r_p & M = M_{eq} \\
 & r = 0 & \dfrac{\partial M}{\partial r} = 0
\end{array}
$$

Grain Velocity and Cycle Time

Knowing the grain circulation rate ($\dot{m}_p$), which is identical to the feed rate of grain for continuous drying, the grain velocity can be determined from:

$$V_p = \dot{m}_p/(\rho_b(1-\varepsilon)A) \quad (5)$$

The dwell time in the spout region is calculated as follows:

$$t_s = H_s/V_{p,s} \quad (6)$$

where H_s and $V_{p,s}$ are, respectively, the spout height and the grain velocity, which is assumed constant throughout the spout region. Similar to Eq. (6), the time taken by the grain in the downcomer can be determined corresponding to the bed height and grain velocity in the downcomer. Since the proportion of time spent by a grain in the spout is insignificant compared with that spent in the downcomer, cycle times can thus be deduced from grains flowing in the downcomer.

The dryer can be assumed to consist of a series of two-dimensional spouted bed sub-dryers in direction of its longitudinal length (Figures 2

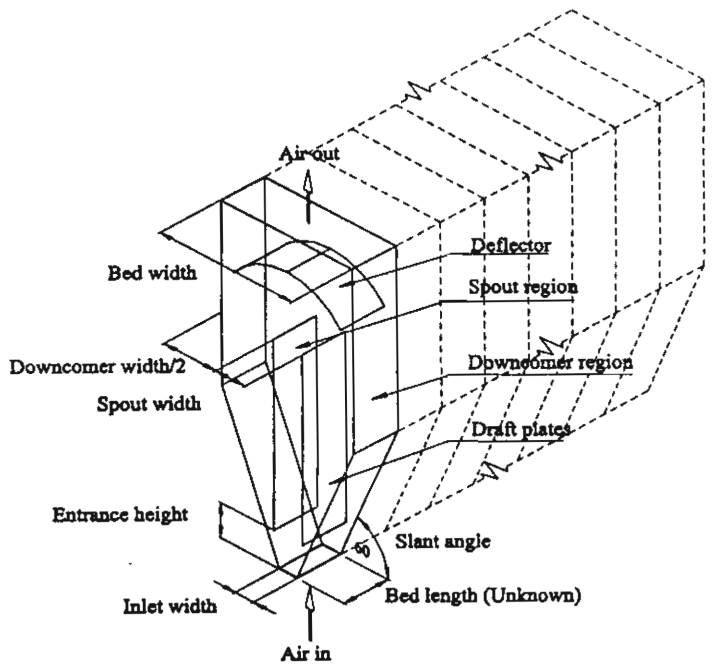

Figure 2. Schematic diagram of typical sub-dryers connected in series

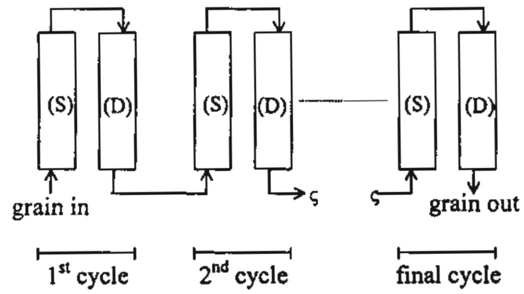

Figure 3. Schematic of grain circulation of two regions. (*S*—spout region, *D*—downcomer region).

and 3). The velocity of grain flowing through each sub-dryer as expressed in Eq. (5), is related to the grain circulation rate ($\dot{m}_p$) and the corresponding cross-sectional area of each region where the grains flow through. Kalwar and Raghavan (10) have found a generalized equation that predicts the grain circulation rates in a two-dimensional spouted bed. By substituting a known grain circulation rate (feed rate) into Kalwar and Raghavan's equation, a length of bed, which is equivalent to the length of a typical sub-dryer was determined. When the length is multiplied by a width of each region, the cross-sectional area corresponding to each region is obtained.

Heat Transfer Coefficient

Many empirical correlations are available in the literature for the estimation of gas to particle heat transfer coefficient (Whitaker (17), Bandrowski and Kaczmarzyk (18) and Rowe and Claxton (19)). These correlations have been developed using many different types of equipment. In the present study and based on preliminary screening simulation, the correlation of heat transfer over a single sphere studied by Whitaker (17) was selected to obtain an expression of the heat transfer coefficient for the spout region. An empirical overall bed heat transfer coefficient for a two-dimensional spouted bed given by Kudra et al. (20) is used to estimate the convective heat transfer coefficient for the downcomer region.

The heat transfer area of particles per unit bed volume for each region is obtained from:

$$a_p = 6(1-\varepsilon)/D \quad (7)$$

where the value of ε for the spout region is 0.98 and 0.40 for the downcomer region; both values are typical of pneumatic transport and fixed beds, respectively.

Diffusion Coefficient

The effective diffusion coefficient, D, is determined by regression analysis from the experimental data of Poomsaad et al. (21) and is given by:

$$D = 5.68033E - 6\exp(-3445.66/T_{abs}) \tag{8}$$

Air Leakage Rates from the Spout to Downcomer

In the present model, the main difficulty that arises is predicting how the gas divides itself between the spout and downcomer. There is no accurate information available on the air leakage from the spout to downcomer for a continuous spouted bed dryer. With the experimental results of batch drying of corn in a two-dimensional spouted bed carried out by Janevijitsakul (22), an empirical curve fit was obtained. It was found that the air leakage ratio depended on the specific airflow rate, SPA (mass ratio of circulated air to dry grains in bed), and the corresponding correlation can be expressed as follows:

$$\text{Air leakage ratio} = 2212.56\text{SPA} - 10.7829 \tag{9}$$

where the air leakage ratio is the mass ratio of air leakage from the spout to the downcomer to total circulated air.

Average Moisture Content

The average moisture content $\overline{M}(t)$ of the paddy kernel is obtained by integrating $M(r, t)$ over the sphere volume.

$$\overline{M}(t) = \frac{4\pi}{V}\int_0^{R_p} r^2 M(r, t)\,dr \tag{10}$$

Constrains of Evaporation Rate

Low mass ratio of grain-to-air especially in the downcomer often leads to overestimation of the drying rates and may cause the evaporation rate more than evaporative capacity of the air. Consequently, the temperature and humidity of air exiting each elementary thin layer need to be checked to see if it is feasible. Once, the state point is not feasible (if the relative humidity is higher than 100%), the excess moisture must be removed from the air by condensation process to converge to a relative humidity of 100% and is then returned into the grain kernel. The temperature and humidity of air corrected for the excess moisture transfer are calculated by the energy equation reported by Thomson et al. (23) and Soponronnarit (24) as follows.

$$c_a T_o + W_o(2502 + c_v T_o) + Rc_{pw}T_o = c_a T_f + W_f(2502 + c_v T_f) + Rc_{pw}T_f \tag{11}$$

where

R = dry mass ratio of grain to air, kg/kg
$= G_p/G_a$

and subscripts o and f refer to non-feasible and corrected conditions of air, respectively.

We can substitute W_f with the function of T_f and then using Newton-Raphson technique for the above equation, T_f and W_f will be obtained. To determine the corrected average moisture content, the following equation is used.

$$\overline{M}_f = \overline{M}_o + (W_f - W_0)/R \tag{12}$$

After condensation we have to push the excess moisture, which is equal to $\overline{M}_o - \overline{M}_f$, back to each interior node inside grain kernel. To simplify the procedure, the nodal moisture contents are recalculated by dividing the excess moisture according to the weight of grain accompanied by each node.

Residence Time Distribution (RTD) of Grains

The aforementioned model is valid for a continuous spouted bed which approaches plug flow, but in reality, the flow pattern of grains in real system does not conform exactly to the postulate of the ideal plug flow. The model can be extended to cover a real system by incorporating an RTD function, which indicates how far the behavior of grain deviates from the ideal behavior and how long different grains remain in a dryer. The experiment was conducted to determine the RTD of paddy in a prototype spouted bed dryer as shown in Figure 4 as well as to determine the appropriate RTD model for using in the model. The experimental results indicated good agreement between RTD obtained from experiments and those determined by units-in-series model (Levenspiel (25)), which views the particles flowing through a series of equal-size well-mixed units. More details of experimental results will be discussed in the main section of result and discussions. The RTD model given by Levenspile (25) is modified for use in this model as follows:

$$E(\theta(j)) = \frac{N(N\theta(j))^{N-1}}{(N-1)!}\exp(-N\theta(j)) \tag{13}$$

where E = residence time distribution function; $j = 1, 2, \ldots, j$th cycle; $\theta(j) = j \times$(cycle time in a typical sub-dryer/mean residence time); N = number of typical sub-dryer in series = mean residence time/cycle time in a typical sub-dryer.

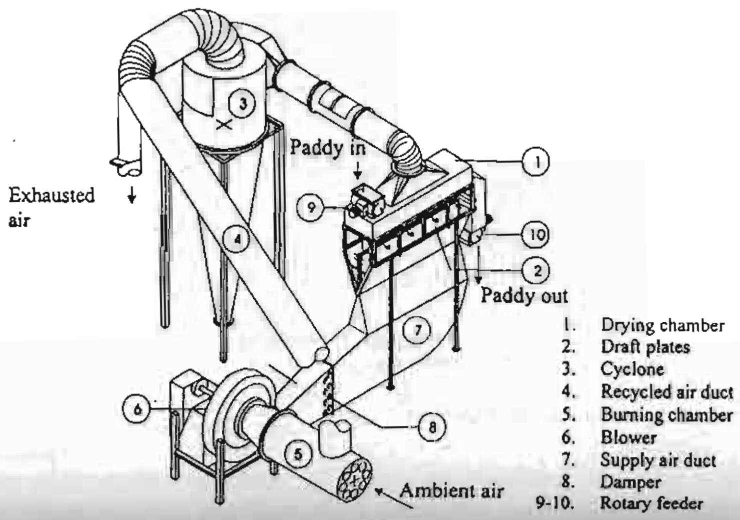

Figure 4. Schematic diagram of the overall experimental set-up.

If this is combined with the relevant average moisture content of grains ($\overline{M}$) at the end of each cycle, the average moisture content of a statistical population of the grains can be determined using Eq. (14), the moisture content of individual grains being, of course, different because of the RTD.

$$\overline{\overline{M}} = \int_0^{\infty} \overline{M}(j)E(j)\,dj \tag{14}$$

where $j = 1, 2, \ldots, j$th cycle; $\overline{M}$ = average moisture content at ending of each cycle; $\overline{\overline{M}}$ = average moisture content of statistical population of grains in continuous process.

The Exit Air Conditions

The exit air temperature and humidity of each sub-dryer are the mixed conditions of the air leaving the spout and downcomer regions.

Properties and Thermodynamics Equations

Expressions for properties of product and thermodynamics equations obtained from literature for paddy and air-water system are listed in Tables 1 and 2.

SOLUTION ALGORITHM

For modeling drying mechanism, we consider that the dryer is represented as a series of sub-dryers (Figure 2). Grains at a constant

Table 1. Properties Used for Simulation

Eqn.#	Property	Expression	Ref.	Unit
15	λ	$(2502 - 2.386T)(1 + 2.496\exp(-21.733M)) \times 10^3$	(26)	J/kg
16	M_{eq}	$[\ln(1-RH)/(c_1 T_{abs})^{1/c_2}]/10$ $c_1 = -3.146 \times 10^{-6}$ $c_2 = 2.464$	(27)	kg/kg
17	c_{pw}	$1.11 \times 10^3 + 44.8(M/(1+M))$	(26)	J/kg K
18	ρ_b	$552 + 282M$	(27)	kg/m^3

Table 2. Thermodynamic of Air and Water Systems (28,29)

Eqn.#	Property	Expression	Unit
19	RH	$RH = 101.3W/(0.62189\ P_{vs} + W\ P_{vs})$	Decimal
20	P_{vs}	$P_{vs} = 100\exp(27.0214 - 6887/T_{abs} - 5.31\ \ln(T_{abs}/273.16))$	Pa
21	c_a	$c_a = 1.00926 \times 10^{3} - 4.0403 \times 10^{-2}T + 6.1759 \times 10^{-4}T^2 - 4.097 \times 10^{-7}T^3$	J/kg K
22	k_a	$k_a = 2.425 \times 10^{-2} + 7.889 \times 10^{-5}T - 1.790 \times 10^{-8}T^2 - 8.570 \times 10^{-12}T^3$	W/m K
23	ρ_a	$\rho_a = 101.325/(0.287T_{abs})$	kg/m^3
24	μ_a	$\mu_a = 1.691 \times 10^{-5} + 4.984 \times 10^{-8}T - 3.187 \times 10^{-11}T^2 + 1.319 \times 10^{-14}T^3$	kg/m s
25	c_v	$c_v = 1.883 \times 10^{3} - 1.6737 \times 10^{-1}T + 8.4386 \times 10^{-4}T^2 - 2.6966 \times 10^{-7}T^3$	J/kg K
26	c_w	$c_w = 2.8223 \times 10^{3} + 11.828T - 3.5043 \times 10^{-2}T^2 + 3.601 \times 10^{-5}T^3$	J/kg K

circulation rate, which is equal to the feed rate, alternately move between the spout and downcomer regions of each sub-dryer until they exit at the bottom of dryer as shown in Figure 3. Since the processes occurred in the spout and downcomer regions substantially influence each other, to better understand the mechanism of drying, the model explicitly accounts for the separate contributions of processes occurring in both regions. The shorter the cycle time the higher the number of sub-dryers will be attained at the relative mean residence time. The conditions of the grains leaving one region are used as input conditions for the grains entering the other region. In a dryer, grain passes through a succession of sub-dryer, the grain conditions from one sub-dryer are carried over to the next, whereas the inlet air conditions can be specified the same for each sub-dryer. The procedure of solution of the governing equations involves the following steps:

1. Because the dryer employs exhaust air recycle, the humidity of inlet air will be elevated above the ambient and the solution must be found iteratively. Thus at the start, the humidity of inlet air needs to be assumed to initiate the simulation.
2. The spout region is considered to consist of a group of elementary thin layers stacked one upon the other. For a given depth of thin layer and a fixed velocity of grain, one can automatically determine a required time step. By applying the diffusion drying equation (Eq. (4)), moisture profiles inside the kernel and change in average moisture content respect to a given time step are determined. The equation is solved numerically using the well-known Crank-Nicholson implicit method.
3. Knowing the inlet air and grain conditions of any given layer, final conditions are calculated at the end of a required time step by solving Eqs. (2) and (3) using the 4th Runge-Kutta method. The outlet air humidity can be determined with mass balance equation (Eq.(1)). The entire procedure is repeated for subsequent layers until reaching the top layer of spout height.
4. The grain conditions at the exit of the spout region are specified as the inlet conditions for the downcomer region. The calculation starts at the elementary thin layer at the top of the downcomer region. An iterative solution is necessary because sufficient initial conditions are not known to simulate its performance directly. At the top of the downcomer, the conditions of drying are not known, and at the bottom the conditions of grain are not known. In this situation, the conditions of inlet air are used as the initial guessed conditions and applied to each elementary thin layer in order to determine the exit conditions of air and grain for a relative elementary thin layer. However, we expect that drying process does not occur instantaneously when grains fall on the bed of downcomer because

the grain surface is still extremely dry due to an exposure to a high temperature air in the spout. Thus, we assume the internal moisture has to be conveyed to the grain surface by diffusion during the downward motion of the grains. This allows moisture redistribution inside the grain kernel without moisture removal, which is defined as a tempering process, but heat transfer between air and grains is still possible. As soon as the surface moisture content of grain is higher than the equilibrium value, determined by the air temperature and humidity, drying will resume.

5. For tempering process, to determine change in moisture profile inside a grain kernel, diffusion Eq. (4) is applied with the boundary condition at grain surface that is $\partial M/\partial r = 0$ and change in air and grain temperatures at the end of a given time step are obtained by setting $dM/dy = 0$ in Eq. (2) and then solving Eqs. (2) and (3) using the 4th Runge-Kutta method. However, cooling of the air, of which mass is substantially less compared to mass of grains in bed, by its passage through the layers may cause the air approaching to the state point that the air is unable to carry moisture anymore (overadsorbtion capacity). This leads to water to condense onto the grain surfaces. Once this happens, Eqs. (11) and (12) are applied to correct the air temperature, humidity and moisture content. The condensed water will remain near the grain surface. Furthermore, the saturated air after condensation is unable to remove moisture from a subsequent layer. Consequently, tempering process will take place for the next layers.

6. For drying process, in the manner analogous to that of the spout region, four differential equations, i.e., Eqs. (1)–(4) are solved simultaneously by numerical method. Constrains of evaporative rate is also needed to be checked, and Eqs. (11) and (12) are employed if necessary to correct air and grain conditions. Then, the final conditions of air for a given elementary thin layer are obtained.

7. The final conditions of air throughout the bed accomplished by procedure in Steps 5 and 6 are now initialized to the conditions of the next iteration while the conditions of grain are remained the same as the beginning. The entire procedure is repeated until the solution is converged.

Return to Step 2 for the grain moving to the next sub-dryer (next cycle). The final grain conditions at the bottom layer of the downcomer region become the initial conditions of the spout region for the next sub-dryer. The calculations are repeated until reaching the end of mean residence time. Repeat Steps 1 to 7 until the difference between assumed and calculated humidity of inlet air is within a specified tolerance. To incorporate with RTD function, the calculations are subsequently extended to three times of the mean residence time to make sure that almost grains do not remain in the dryer and then apply Eqs. (13) and (14) to determine the average moisture content of a statistical population of the grains.

RESULTS AND DISCUSSION

Residence Time Distribution

The experiment was conducted to predict the behavior of a continuous spouted bed dryer as shown in Figure 4 that can be characterized by RTD of grains. The opaque circular symbols as presented in Figure 5 show the results of the experiment on the RTD function of paddy at a constant feed rate of 3500 kg/h. It is clearly seen that the residence times of individual grain vary considerably. However, the RTD curve appeared to have longer tail at the right side but it approximated a normal distribution curve. This means a proportion of grains leaving the bed approximates to that of the rest in the bed after a mean residence time. The spread of residence time about the mean indicated some degree of backmixing in a continuous system and reflected that dryer behavior deviated from ideal plug flow. By a comparison with the RTD curve corresponding to units-in-series model (Levenspiel (25)) represented by a solid line in Figure 5, it shows that the Levenspiel RTD model has good agreement with the experimental RTD.

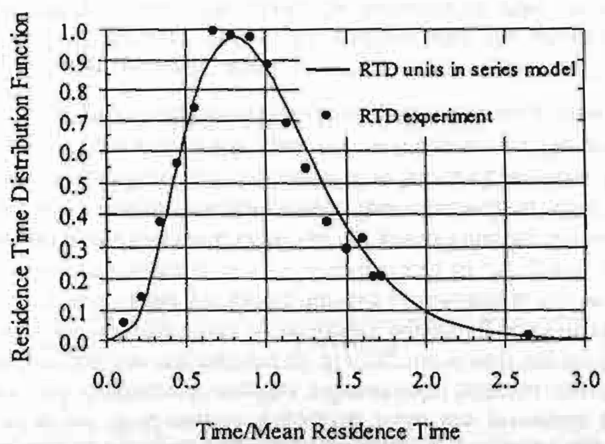

Figure 5. Residence time distribution of paddy in a continuous spouted bed at a constant feed rate of 3340 kg/h and a hold-up of 315 kg.

Hence, the RTD model given by Levenspile (25) is selected for using in modeling the drying of grain in a continuous spouted bed.

Validation of Model

The mathematical model was validated with the experimental results of continuous drying of paddy in an industrial-scale spouted bed dryer (Figure 4) proposed by Madhiyanon et al. (12). The operating conditions and the bed geometry are summarized in Tables 3 and 4, respectively.

Table 3. Operating Conditions for Model Validation

	Run No.				
Parameter	1	2	3	4	5
Feed rate (kg/h)	2370	2400	3160	3280	3550
Inlet air temperature (°C)	152	159	154	156	160
Ambient temperature, db/wb (°C)	37/30	34/28	33/32	30/27	35/27
Inlet grain temperature (°C)	37	34	34	35	35
Mean residence time (min)	6.0	5.3	6.4	5.3	5.2
Initial moisture content (%d.b.)	22.1	25.0	29.4	28.2	22.8
Hold-up (kg)	240	210	335	290	310
Grain diameter (mm)	3.5	3.5	3.5	3.5	3.5
Total air flow rate (kg dry/s)	1.45	1.45	1.40	1.45	1.30
Air leak-off rate into the downcomer (%)	5	8	2	3	2
Recycled air ratio (%)	75	74	76	72	75

Table 4. Geometric Parameters of the Spouted Bed

	Run No.				
Bed Dimensions	1	2	3	4	5
Spout height (m)	1.3	1.3	1.3	1.3	1.3
Entrance height (m)	0.125	0.125	0.125	0.125	0.150
Spout width (m)	0.06	0.06	0.06	0.06	0.06
Bed width (m)	0.60	0.60	0.60	0.60	0.60
Bed height (m)	0.65	0.60	0.85	0.80	0.80
Inlet width (m)	0.04	0.04	0.04	0.04	0.04
Slant angle (degrees)	60	60	60	60	60

Table 5 presents the results of five runs of experiment. The average errors of moisture losses predicted by the plug flow model and the model incorporating with RTD were 14.3% and 12.0%, respectively. There is no significant difference between the final moisture content obtained from the plug flow model and the model with RTD taken into account. Final grain temperatures predicted by the simulation differed from the experimental values by a mean of 8.4%.

The causes of discrepancies of final grain conditions are not exactly clear because for a two-region model as the present study, the final moisture and grain temperature are affected by a variety of processes that exist during both in the spout and downcomer. The processes occurring in both regions concern with several parameters, i.e., airflow rate, grain velocity, heat and diffusion coefficients. Therefore, it is difficult to investigate the cause of non-matching results between the experiments and simulations by recognizing

Table 5. Validation of Model for Continuous Drying of Paddy

	Run No.				
Description	1	2	3	4	5
	Experiment				
Initial m.c (%d.b.)	22.1	25.0	29.4	28.2	22.8
Final m.c (%d.b.)	17.1	19.7	25.0	23.3	19.0
Final grain temp. (°C)	71	68	67	67	68
Spec. energy consumption (MJ/kg water evap.)	4.4	5.2	3.5	3.8	–
	Simulation				
Final m.c. (%d.b.)					
Plug flow	17.9	20.3	24.7	24.1	19.8
Plug flow integrating with RTD	17.9	20.4	24.7	24.1	19.3
Final grain temp. (°C)	81	78	63	63	67
Spec. energy consumption with RTD (MJ/kg water evap.)	5.6	5.5	4.0	4.6	4.4
Error in moisture loss (%)					
Plug flow	−16.0	−11.3	6.8	−16.3	−21.1
Plug flow integrating with RTD	−16.0	−13.2	6.8	−16.3	−7.9
Error in final grain temp. (%)	14.0	14.7	−6.0	−6.0	−1.5
Error in spec. energy consumption (%)	27.3	5.8	14.3	21.1	–

$$\text{Error} = \frac{\text{Sim} - \text{Expt}}{\text{Expt}} \times 100\%$$

temperature difference between grain and air. Both kinetics of moisture content and grain temperature are helpful in the design of grain drying process especially when they are considered as the parameters to control the product quality.

Limitation of the Dryer

According to the study of Madhiyanon et al. (12), achieving low moisture content was limited by a short mean residence time due to insufficient dryer length and hence the grain cannot be dried to a desirable level for safe storage. Therefore, in addition to know more information of continuous spouted bed, it was further simulated by extending the dryer length (from 2.1 to 5 m) which resulted in longer mean residence time and thus obtaining lower moisture and higher grain temperature. The result as shown in Figure 6d indicates that the grain moisture content progressively decreases at almost a constant rate without depending on whether the product is being wetted or dried, that is consistent with the experimental results of Wetchakama et al. (11) and Ngugen (5). This may allow the possibility of the spouted bed dryer to dry products with low moisture content that are usually difficult to dry. Drying products at low moisture content with interaction between drying in the spout and moisture relaxation in the downcomer could help to additionally accelerate moisture removal as compared to drying with conventional drying processes. The grain temperature (Figure 6d) first sharply increases and thereafter it gradually increases as grain approaches to drying air temperature. However, it is of particular interest for agro-products that would be damaged by excessive grain temperature if grains stay in a dryer too long as presented in Figure 6d. This may be a limitation of a spouted bed dryer that drying grains in one pass through a dryer is practically impossible and this is also supported by the work of Ngugen (6).

Temperature Distribution and Heat Transfer

Figure 7 shows the grain and air temperatures predicted by the mathematical model, against bed height of the downcomer, for a counter-flow bed under the conditions of low airflow and warm inlet grain. It appears in Figure 7 that the air in the downcomer attains thermal equilibrium with the grains within a few centimeters of its entry into the bed. This is also found in the results of Madhiyanon et al. (13). This evidence may rise an idea for diminishing the complexity of solution scheme for the downcomer by

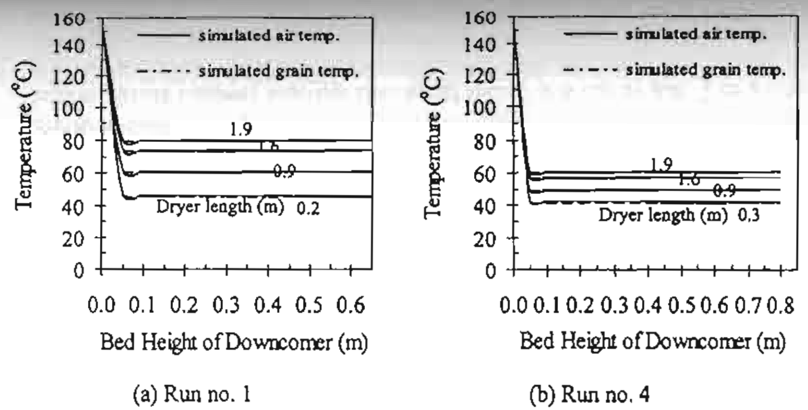

Figure 7. Temperature distribution of air and grain inside the downcomer bed.

assuming isothermal bed and thermal equilibrium condition between air and grains in the bed.

Moisture Content Profiles Regarding to Processes Occurring in the Downcomer and Spout Regions

Figure 8 shows the simulation moisture content distribution inside a grain kernel during grain movement in the downcomer. Moisture profiles at the beginning of the downcomer period, which are identical to those at the end of preceding spouting period, present the existence of relative large moisture gradients inside the grain kernel. Hence the air-grain interface resistance regarding to grain exposure to a high airflow and high temperatures in the spout is much lower than the internal mass transport resistance of the material leading to development of moisture gradient within the grain.

The simulation results illustrate that there was only the evidence of moisture relaxation inside the grain kernel with the absence of moisture removal in the downcomer. This is reflected by the decrease of the moisture gradients due to moisture migration from the center to the outer layer by diffusion during grain passage in the downcomer as shown in Figure 8. This may be explained with reference to very low air-to-grain mass ratio in the downcomer that has very little potential for heating and removing moisture from grains, and thus leading to tempering instead of drying. Opposite to

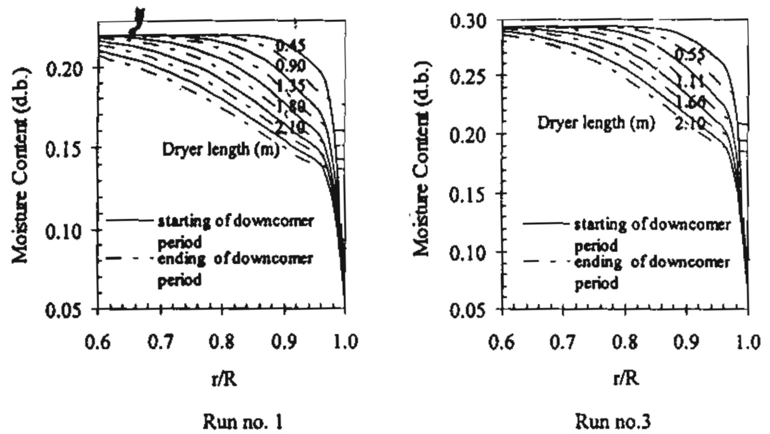

Figure 8. Simulated transient moisture profile inside a paddy kernel during downcomer period at different dryer lengths.

the evidence occurring in the spout region, the changes in moisture content of grain are attributed to evaporation of moisture near grain surface during grain flowing through the spout as indicated by moisture profiles inside grain kernel as presented in Figure 9.

Unlike to the previous work of Madhiyanon et al. (13) that there was no moisture relaxation but gentle drying existed almost all of the time spent in the downcomer. This is not surprising and could be reasoned that the air leakage rates from the spout to the downcomer of the previous work were substantially high compared to those of the present work, i.e., about ten to twenty orders of magnitude. The reason was that airflow required to sustain spouting stable of paddy in present work was very low compared with that required for corn in the former work. Thus, air leakage ratio computed by Eq. (9) was much less for this case.

Milling Yields and the Possible Strategy for Grain Drying in Spouted Bed

Madhiyanon et al. (13) reported that no serious loss in milling quality in terms of head rice yield and whiteness was found in their experiments. High temperature up to 160°C can be used without any adverse effect on quality. This is reasoned that a short residence time of individual grain remaining in their dryer could not affect grain color, and moisture

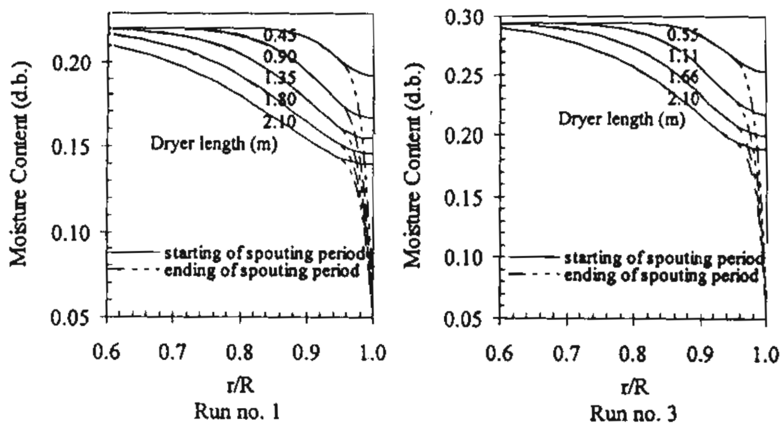

Figure 9. Simulated transient moisture profile inside a paddy kernel during spouting period at different dryer lengths.

redistribution during the rest period of downcomer allowed grains to relieve the stresses developed within the kernel, leading to insignificant effect on head rice yield. For longer residence times, in order to obtain lower moisture content, i.e., safe storage level, grain quality may be affected as shown in Figure 6d that grain temperature increases continually. To maintain quality, the operation may be divided into two-stage drying with long enough period of tempering in-between.

CONCLUSIONS

A mathematical model was developed to predict the performance of a continuous spouted bed dryer with air recycle. The model was validated with the experimental results for continuous drying of paddy. The model computes changes in moisture content, air and grain temperatures and energy utilization. In this study, RTD was used to characterize the behavior of dryer. The experimental RTD indicated that behavior of the dryer deviated from ideal plug flow. There is no significant difference in predicted final moisture content whether the model includes RTD or not. The average percentage error in moisture loss was 14.3% for the plug flow model and 12.0% for the model incorporating RTD. The average percentage error in grain temperature and specific energy consumption were 8.4% and 17.0%, respectively. Simulation results indicated that under substantially low air leakage from the spout to the downcomer, alternating operation of a spouted bed leads to a major part of heating and drying taking place in the spout with negligible moisture removal in the downcomer. The tempering time in the downcomer facilitates evaporation of moisture in the spout and leads to an almost constant drying rate. As expected, thermal equilibrium condition of air and grains in the downcomer was observed and may be used to simplify the model. Simulation results indicate that it is difficult or impossible to achieve both high product quality and low moisture content for safe storage simultaneously by a single pass of drying through a continuous spouted bed dryer. Hence, multistage drying would be more appropriate.

NOMENCLATURE

Symbols

A	Cross-sectional area of elementary thin layer (m^2)
a_p	Surface area of particles per unit bed volume (m^2/m^3)
c	Specific heat (J/kg K)
c_p	Specific heat of dry particles (J/kg K)
c_{pw}	Specific heat of wet product (J/kg K)
D	Effective diffusion coefficient (m^2/s)
D_p	Equivalent particle diameter (m)
E	Residence time distribution function (–)
G	Dry mass flux (kg/m^2s)
h	Convective heat transfer coefficient (J/m^2 K)
H_s	Spout height (m)
k_a	Thermal conductivity of dry air (W/m K)
M	Moisture content (decimal d.b.)
$\overline{M}$	Average moisture content (decimal d.b.)
$\overline{\overline{M}}$	Average moisture content of statistical population of grains in continuous process (decimal d.b.)
$\dot{m}$	Dry mass flow rate (kg/s)
P_{vs}	Saturated vapor pressure (Pa)
r	Radial distance from center of sphere (m)
R	Dry mass of grain to air ratio (kg/kg)
R_p	Equivalent particle radius (m)
RH	Relative humidity (decimal)
SPA	Specific airflow rate (kg air/kg grain-s)
t	Time (s)
T	Temperature (°C)

V_p	Velocity of particles (m/s)
V	Volume of a single particle (m^3)
W	Air humidity (kg water vapor/kg dry air)

Greek letters

ε	bed porosity (–)
ρ_a	density of dry air (kg/m^3)
ρ_b	bulk density of particles (kg/m^3)
λ	heat of evaporation (J/kg)
θ	time dimensionless (–)

Subscripts

a	air
abs	absolute
amb	ambient
d	downcomer region
eq	equilibrium
f	corrected condition
in	initial
mix	mixing
o	infeasible condition
p	particle
s	spout region
v	vapor
w	water

ACKNOWLEDGMENT

The authors would like to thank the Thailand Research Fund for financial support.

REFERENCES

1. Becker, H.A.; Sallans, H.R. Drying Wheat in a Spouted Bed. Chem. Eng. Sci. **1960**, *13*, 97–112.
2. Zuritz, C.A.; Singh, R.P. In *Simulation of Rough Rice Drying in a Spouted Bed*, *Drying'82*, Mujumdar, A.S. Ed.; McGraw-Hill: Hemisphere, New York, 1982; 239–247.

3. Zahed, A.H.; Epstein, N. Batch and Continuous Spouted Bed Drying of Cereal Grains: The Thermal Equilibrium Model. Can. J. Chem. Eng. **1992**, *70*, 945–953.
4. Zahed, A.H.; Epstein, N. On the Diffusion Mechanism During Spouted Bed Drying of Cereal Grains. Drying Technol. **1993**, *11*(2), 339–354.
5. Nguyen, L.H. *Evaluation of a Modified Spouted Bed Dryer for High Moisture Grain Drying*, Ph.D. Thesis, University of New South Wales, Australia, 2000.
6. Nguyen, L.H.; Driscoll, R.H.; Srzednicki, G. Drying of High Moisture Content Paddy in a Pilot Scale Triangular Spouted Bed Dryer. Drying Technol. **2001**, *19*(2), 375–387.
7. Jumah, R.Y.; Mujumdar, A.S.; Raghavan, G.S.V. A Mathematical Model for Constant and Intermittent Batch Drying of Grains in a Novel Rotating Jet Spouted Bed. Drying Technol. **1996**, *14*(3–4), 765–802.
8. Jumah, R.Y.; Mujumdar, A.S.; Raghavan, G.S.V. A Mathematical Model for Constant and Intermittent Batch Drying of Grains in a Novel Rotating Jet Spouted Bed. In *Mathematical Modeling and Numerical Techniques in Drying Technology*, Mujumdar, A.S., Turner, I., Eds.; Marcel Dekker, Inc: New York, Basel and Hong Kong, 1997; 339–380.
9. Kalwar, M.I.; Raghavan, G.S.V. Batch Drying of Shelled Corn in Two-Dimensional Spouted Beds with Draft Plates. Drying Technol. **1993**, *11*(2), 339–354.
10. Kalwar, M.I. and Raghavan, G.S.V. Circulation of Particles in Two-Dimensional Spouted Beds with Draft Plates. Powder Tech., **1993**, *77*, 233–242.
11. Wetchacama, S.; Soponronnarit, S.; Swasdisevi, T.; Panich-ing-orn, J.; Suthicharoenpanich, S. In *Drying of High Moisture Paddy by Two-Dimensional Spouted Bed Technique*, Proceedings of the First Asian-Australian Drying Conference (ADC'99), Bali, Indonesia, Oct. 24–27, 1999; 300–307.
12. Madhiyanon, T.; Soponronnarit, S.; Tia, W. Industrial-Scale Prototype of Continuous Spouted Bed Paddy Dryer. Drying Technol. **2001**, *19*(1), 207–216.
13. Madhiyanon, T.; Soponronnarit, S.; Tia, W. A Two-Region Mathematical Model for Batch Drying of Grains in a Two-Dimensional Spouted Bed. Drying Technol. **2001**, *19*(5). (In press)
14. Mujumdar, A.S. In *Spouted Bed Technology: A Brief Review, Drying'84*, Hemisphere: Washington, 1984; 151–157.

15. Pallai, E.; Szentmarjay, T.; Mujumdar, A.S. Spouted Bed Drying, Ch.13. In *HandBook of Industrial Drying*, Vol. 1; Mujumdar, A.S., Ed.; Marcel Dekker, Inc.: New York, 1995, 453–488.
16. Passos, M.L.; Mujumdar, A.S.; Raghavan, G.S.V. Spouted Bed Drying. In *Principles and Design Consideration in Drying*, Vol. 4; Mujumdar, A.S., Ed.; Hemisphere: New York, 1987; 359–398.
17. Whitaker, S. Force Convection Heat Transfer Correlations for Flow in Pipes, Past Flat Plates, Single Cylinders, Single Spheres and for Flow in Packed Beds and Tube Bundles. AIChE **1972**, *18*(2), 361–371.
18. Bandrowski, J.; Kaczmarzyk, G. Gas to Particle Heat Transfer in Vertical Pneumatic Conveying of Granular Materials. Chem. Eng. Sci. **1978**, *33*, 1303–1310.
19. Rowe, P.N.; Claxton. K.T. Heat and Mass Transfer from a Single Sphere to Fluid Flowing through an Array. Trans. Inst. Chem. Eng. **1965**, *43*, T231–T331.
20. Kudra, T., Mujumdar, A.S.; Raghavan, G.S.V. Gas-to-Particle Heat Transfer in Two-Dimensional Spouted Beds. Int. Comm. Heat and Mass Transfer **1989**, *16*(5), 731–741.
21. Poomsaad, N.; Soponronnarit, S.; Therdyothin, A. In *Diffusion Models of Paddy Drying by Fluidization Technique*, Proceeding of the 14th Memorial CIGR World Congress 2000, Japan, Nov.28–Dec.1, 2000, 777–782.
22. Janevijitsakul, K. *Two-Dimensional Spouted Bed Corn Drying*, M. Eng. Thesis, King Mongkut's University of Technology Thonburi, Thailand, 2000.
23. Thompson, T.L.; Peart, R.M.; Foster, G.H. Mathematical Simulation of Corn Drying: A New Model. Trans. ASAE **1968**, *11*(4), 582–586.
24. Soponronnarit, S. Energy Model of Grain Drying System. ASEAN Journal on Science and Technology for Development **1988**, *5*(2), 43–68.
25. Levenspiel, O. *Chemical Reaction Engineering*, Ch. 9, 2nd Ed.; John Willey & Sons: New York, London, Sydney and Toronto, 1972, 253–315.
26. Brooker, D.B., Bakker, F.W.; Hall, C.W. *Drying and Storage of Grain and Oilseed.* AVI: New York, 1992; Appendix E.
27. Laithong, C. *Study of Thermo-Physical Properties of Rough Rice*, M. Sci. Thesis, King Mongkut's Institute of Technology Thonburi, Thailand, 1987.
28. Mujumdar, A.S. *Handbook of Industrial Drying*, 2nd Ed.; Marcel Dekker, Inc.: New York, 1995; Appendix.

29. Pakowski, Z.; Bartczak, Z.; Strumillo, C.; Stenstrom, S. Evaluation of Equations Approximating Thermodynamic and Transport Properties of Water, Steam and Air for Use in CAD of Drying Processes. Drying Technol. **1991**, *9*(3), 753–773.
30. Meeso, N.; Soponronnarit, S.; Wetchacama, S. In *Evaluation of Drying System Performance in Rice Mills*, Proceeding of the 19th ASEAN Seminar on Postharvest Technology 1999, Vietnam, Nov. 8–12, 1999; 286–295.
31. Soponronnarit, S.; Prachayawarakorn, S. In *Recent Research and Development Work on Paddy Drying in South-East Asia*, Proceeding of the 20th ASEAN Seminar on Postharvest Technology 2001, Thailand, Sep. 11–14, 2001.

DESORPTION ISOTHERMS AND DRYING CHARACTERISTICS OF SHRIMP IN SUPERHEATED STEAM AND HOT AIR

Somkiat Prachayawarakorn,[1] Somchart Soponronnarit,[2] Somboon Wetchacama,[2] and Donrudee Jaisut[2]

[1]Faculty of Engineering and
[2]School of Energy and Materials,
King Mongkut's University of Technology
Thonburi, Suksawad 48 Rd., Tungkru,
Bangkok 10140, Thailand

ABSTRACT

Desorption isotherms for shrimp were determined at the temperatures of 50, 60, 70 and 80°C. Amongst the moisture equilibrium predictions between the BET and GAB models, the latter has a better predictable capability. The GAB parameters are correlated with the temperatures by the Arrhenius expression. Drying characteristics of shrimp in drying media at the temperature range of 120–180°C for superheated steam and of 70–140°C for hot air have been examined. Drying rate and effective diffusion coefficient are used to quantify quantitatively the difference between the superheated steam and the hot air dryings. The temperature is more important effect on drying rate and effective diffusion coefficient in the superheated steam than in the hot air. Inversion temperature exists between 140 and 150°C. Comparing to the hot air, the shrimp dried by the superheated steam shows a lower degree of shrimp shrinkage. In addition, product colours are slightly different to those from the commercial sources.

Key Words: Dehydration; Equilibrium moisture content; Inversion temperature; Marine; Quality

INTRODUCTION

Shrimp has long been recognized as a highly priced commodity. To delay the deterioration, raw shrimp has traditionally been dried by sun drying or roasting in the opened air, but in some areas where the sunshine is irregular or insufficient, the dryer is usually used. Production of dried shrimp has been done in a very small-scale level. However, with a considerable increase of its demand both domestic and foreign markets, an increase in production would be needed. This motivates us to explore a way of improving the dried shrimp process providing high drying rate, convenient way, save energy and superior quality. The preferred quality is characterised by red-orange colour and low shrinkage.

The process of dried shrimp can be mainly divided into two categories, boiling the raw shrimps in NaCl solution in order to prevent the growth of microorganisms, i.e., *Bacillus* and *Pseudomonads*, and drying. If the boiling process is done improperly, the survival of microorganisms may be achieved. There are various boiling conditions as recommend by several authors, for instance, at 101°C for 1.5 min (Crawford, 1981) or at 100°C for 3 min (Price, 1997). If the shrimps are boiled for the longer time, then larger quantity of NaCl can penetrate through their cells, so that the shrimps become too salty. Salting of shrimp is achieved by adding about 2–10% salt during the boiling stage. The boiled shrimps are then taken to reduce the moisture content. The method of drying process has different techniques: conduction, convection and radiation. Amongst these techniques, the convective drying is most widely used. High temperature range is likely preferred since the drying time could be reduced, as its main aim, but too high temperature may affect the quality of product.

There has been rather limited work on shrimp drying. Posomboon (1998) reported that the colour and texture for shrimp dried using hot air at the temperatures between 40 and 70°C was found to be insignificantly different. However, when the drying temperatures lied between 100 and 140°C, the colour became poorer and the matter was too tightly contacted

According to the above-mentioned dried shrimp process, it is now very inconvenient in practice. The boiling and drying stages for such typical dried shrimp process can be combined in one unit when the superheated steam is applied. The superheated steam drying has been attracted a wide interest in many applications (Akao, 1983; Salin, 1988; Blasco and Alvarez, 1995; Tarnawski et al., 1996). Earlier studies have illustrated some of advantages of steam drying (Hirose and Hazama, 1983; Stubbing, T.J., 1999; Chen et al., 2000): high drying rates in both constant and falling periods as well as deodorization and/or pasteurisation of products.

The objectives of the present work are: 1) to determine desorption isotherms for shrimp under different temperatures and relative humidity levels; 2) to compare drying characteristics and shrinkage between the superheated steam and hot air dryings; and 3) to compare the colour quality of dried shrimp from the superheated steam drying and the commercial sources. We anticipate that this research will lead us to better understanding for drying characteristics in the superheated steam and hot air and how drying media may affect the qualities.

MATERIALS AND METHODS

Equipment

Figure 1 shows a schematic diagram of the closed loop superheated steam drying system consisting of a mechanical blower, a superheat unit, a batch dryer, a steam generator, pressure gauges and steam conveying pipe lines. Steam generated from the steam generator (No. 4) at 1 bar was flowed through the superheat unit (No. 2) with a capacity of 13.5 kW and it became superheat. The superheated steam was then passed through the small cabinet dryer with a size of 0.3 m × 0.3 m × 0.1 m (No. 3). All quantities of the exhausted steam were eventually re-circulated by the backward-curved blade centrifugal fan (No. 1), controlled by a mechanical speed controller to obtain the desired air flow rate. Thus, energy consumption would be saved proficiently because the outlet steam that still had a very high temperature was not delivered to the atmosphere. Steam velocity was fixed at a value of 1.6 m/s and pressure at the drying chamber was operated constantly at a slightly above atmospheric pressure to ensure that no air leaked into the system. The steam was flowed in parallel direction of wire screens fitted in the dryer. Before running superheated steam for drying shrimps, the hot air was first used for warming up all the units until the temperature reach the

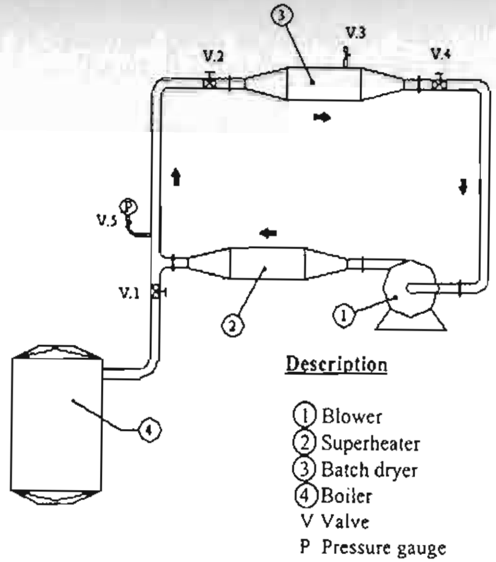

Figure 1. Schematic diagram of superheated steam dryer.

Desorption Isotherm

Raw shrimp samples were cut into an approximate size of 0.5 cm × 0.5 cm × 0.2 cm and then placed in a series of saturated salt solutions under different temperatures to obtain the desired water activity. In this study, the water activity was covered over a range of 0.1 and 0.9 at three temperatures, 60, 70 and 80°C. The samples were weighed periodically on a meter balance (an accuracy of ±0.005) until the change of their mass between weightings was less than 0.05%, indicating that the samples and saturated salt solutions were in equilibrium. In each condition, it was repeated three times. The moisture content of the sample after reaching the equilibrium was determined by a hot air oven at 103°C for 72 h (Anon, 1960).

Shrimp Drying

Raw shrimps (Penaeidae) were dipped into 2% (W/V) NaCl solution for 30 min at room temperature before drying with superheated steam. When the conditions of drying system reached steady state, the samples

were placed on three wire screens in a small drying chamber. Weight was recorded every 15 min. Drying was performed at a steam velocity of 1.6 ± 0.2 m/s and inlet steam temperatures of 120, 140, 160 and 180°C. The moisture content in each wire screen over drying period was less than 5% difference, indicating the uniform flow in the drying chamber. In case of drying shrimps with hot air, the raw shrimps were boiled at the same NaCl concentration as mentioned above for 15 min before drying. In this case, the drying temperatures were set at 70, 90, 120 and 140°C, with the same superficial velocity as the steam case.

In analysis of the drying kinetics, geometry of shrimp was assumed to be a sphere with an equivalent diameter of 18.9 mm and shrimp has an initial moisture content of 455.6% d.b.

Shrinkage Test

For the shrinkage study, the samples of dried shrimp from the superheated steam at 120, 140 and 160°C and the hot air at 120 and 140°C were measured the size by a vernia scale. Percentage of shrinkage calculated by

$$\%\ \text{shrinkage} = \frac{Z_o - Z_t}{Z_o} \times 100 \qquad (1)$$

where Z_o and Z_t are respectively the sizes of shrimp at the beginning and the end of the drying experiment.

Colour Test

The samples of dried shrimp obtained from the superheated steam at different temperatures and from the local markets were taken to determine the colours using a colour meter, Juki JP 7100 p. The colours were represented in "a", "b" and "L" values in Hunter system. 'L' shows the lightness and 'a' represents the redness or greenness whereas 'b' means the blueness or yellowness. The net change of the product colour (ΔE) is calculated by the following equation:

$$\Delta E = [\Delta L^2 + \Delta a^2 + \Delta b^2] \qquad (2)$$

where L, Δa and Δb are the differences of the colours at the beginning and the final.

Modeling of Desorption Isotherms

There are a large number of models available for describing the moisture equilibrium of foods under different water activity levels and temperatures. In this work, the two well-known theoretical isotherm models, the Braunauer, Emmett and Teller (BET) and the Guggenheim, Anderson and de Boer (GAB), were used to fit the desorption results. Such models have the following forms:

$$\text{BET} \qquad M_{eq} = \frac{M_b Y a_w}{(1-a_w)[1+(Y-1)a_w]} \tag{3}$$

$$\text{GAB} \qquad M_{eq} = \frac{M_b S Y a_w}{(1-Sa_w)[1+(Y-1)Sa_w]} \tag{4}$$

where M_{eq} and M_b are the equilibrium moisture content (dry basis decimal) and the moisture content corresponding to the monomolecular layer of water, respectively, a_w is water activity (fraction), Y and S are the constant values of desorption isotherm related to the temperature by the following Arrhenius forms:

$$Y = G\exp(-E/RT_{abs}) \tag{5}$$

$$S = A\exp(-C/RT_{abs}) \tag{6}$$

where E and C are the constant parameters obtained from the experiments, R is the universal gas constant and T_{abs} is the absolute temperature. From Eq. (3), if S is equal to unity, the GAB model is exactly identical to the BET.

The R-square (R^2) and summation of square error (SSE) were used to consider how well the desorption models could explain the experimental results. The SSE is given by

$$\text{SSE} = \sum_{i=1}^{n} (\text{experiment} - \text{observed})^2 \tag{7}$$

Modeling of Drying Kinetics

During the falling rate period, the internal resistance of moisture transfer is an important factor to control the moisture movement inside solids. An effective diffusion coefficient (D_{eff}) is used to describe the drying rate in this period. For a spherical geometry, the solution of Fick's unsteady state equation with suitable boundary and initial conditions can be expressed as (Crank, 1975)

$$\text{MR} = \frac{M(t) - M_{eq}}{M_{in} - M_{eq}} = \frac{6}{\pi^2}\sum_{n=1}^{\infty}\frac{1}{n^2}\exp\left(-\frac{n^2\pi^2 D_{eff} t}{r^2}\right) \tag{8}$$

where M_{eq} is the equilibrium moisture content, M_{in} is the initial moisture content and $M(t)$ is the moisture content at time t (minute) and r is the sphere radius. In case of $D_{eff}t/r^2 < 0.1$, it is essentially necessary to consider all terms in Eq. (8). Thus, 10 terms of this equation were used sufficiently for predicting the values of MR throughout the drying curve.

In calculating the moisture content, we assumed M_{eq} to be zero. In addition, the shrimp size was presumably constant during drying period. The temperature effect on the effective diffusion coefficient is taken into account by the Arrhenius type equation,

$$D_{eff} = D_o\exp(-H/RT_{abs}) \tag{9}$$

where T_{abs}, D_o and H are the absolute temperature of drying media (K), the Arrhenius factor and the activation energy, respectively. D_o is equivalent to the effective diffusion coefficient at the infinite temperature.

RESULTS AND DISCUSSION

Desorptions of Shrimp

Table 1 shows the estimated characteristic constants of desorption isotherms together with the corresponding R^2 and SSE obtained from the nonlinear regression analysis for the BET and GAB models. The GAB model provides better fit to the experimental results with a higher value of R^2 and a lower value of SSE. This is consistent with the works as reported by the several researchers for agricultural commodities (Iglesias and Chirife, 1995; Kechaou and Maalej, 1999; Lopez et al., 2000; Vázquez et al., 2001).

The experimental desorption isotherms at various temperatures and the validation of the models are shown in Figures 2 and 3. It clearly indicates that the temperatures have an influential effect on the water contents at the equi-

Table 1. Non-Linear Regression Analysis of the BET and GAB Models

Models	A	M_b	C	G	E	R^2	SSE
GAB	0.00275	0.0826	15535	5.1278	627.87	0.99	0.002
BET	–	0.0352	–	7.09×10^6	−5995.69	0.79	0.04

librium; an increase in the temperatures results in the lower equilibrium moisture contents at the corresponding values of relative humidity.

As shown in Figures 2 and 3, the GAB model can explain agreeably with the results for all the ranges of the temperatures and the water activity levels considered, but the BET fails to describe the temperature effect on the desorption isotherms.

Moisture Contents

The experimental and predicted moisture contents for the superheated steam shrimp drying at the temperatures of 120, 140, 160 and 180°C are shown in Figure 4 indicating the remarkably lower moisture contents for the higher superheated steam temperatures at the corresponding drying times. The drying times for reducing the moisture content from the beginning to 25% d.b. are approximately 120, 60 and 25 min for the superheated steam at 120, 140 and 160°C, respectively. At the steam temperature of 180°C, although drying time in reducing moisture content to the desired level is the shortest, it is not of particular interest because the surface colour of the dried shrimp is very poor (brown colour) and the dehulling shell from its matter is much more difficulty. As indicated in Figures 4 and 5, the moisture content at the end point for each curve is zero after which the shrimp was

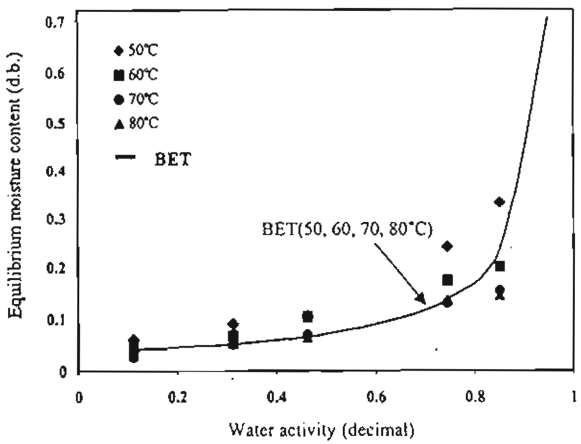

Figure 2. Comparison of equilibrium moisture content of shrimp between experiments and predictions from the BET model.

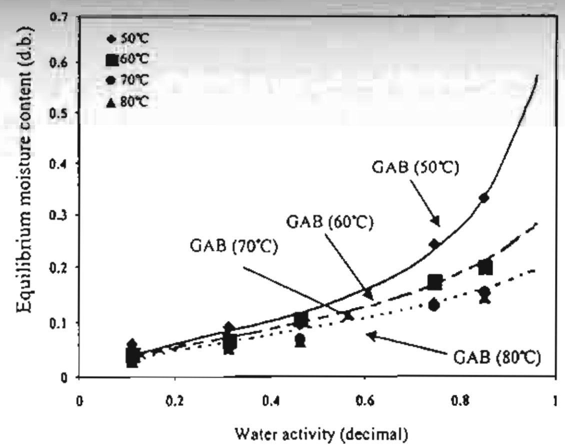

Figure 3. Comparison of equilibrium moisture content of shrimp between experiments and predictions from the GAB model.

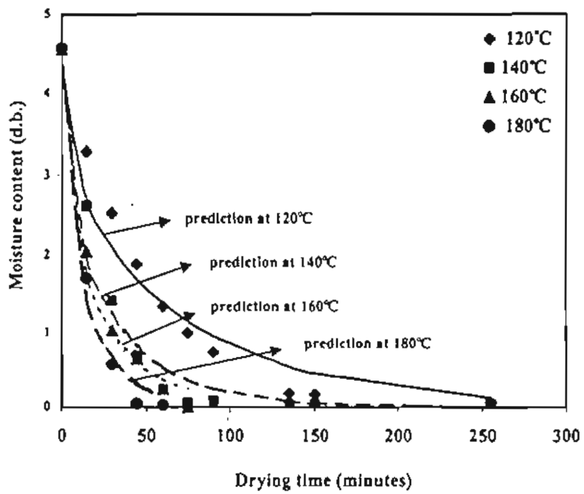

Figure 4. Drying kinetics of shrimp in the environment of superheated steam at different temperatures and the fits of diffusion model.

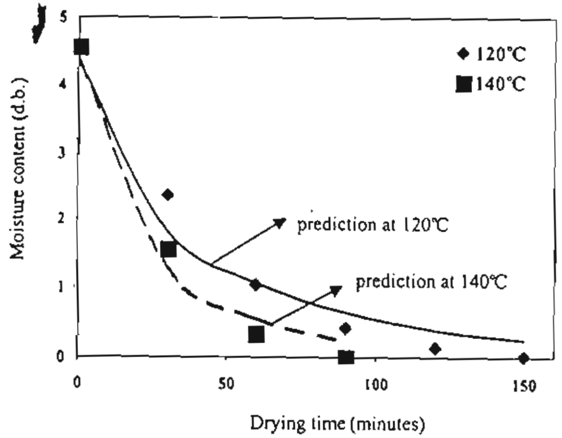

Figure 5. Moisture contents of shrimp in hot air at different temperatures and the fits of diffusion model.

contacted with the drying media for a sufficiently longer period. This was in agreement with the early-mentioned assumption used in calculating the effective diffusion coefficient.

For the hot air shrimp drying, the two drying curves at 120 and 140°C represented in Figure 5 are found to have a similar trend as in Figure 4, showing the exponential decay of moisture content with drying time. Shrimp dried at those temperatures possesses the moisture difference smaller than that dried by superheated steam. For example, at the drying time of 30 min, the moisture differences are 0.79 d.b. for the hot air and 1.11 d.b. for the superheated steam. The reason for this behaviour is probably due to the small temperature difference between the interface and bulk airflow.

The drying times for removing the moisture content to the desired level in the hot air are approximately 110 and 70 min at the temperatures of 120 and 140°C respectively, indicating the decrease of drying time by 36% whereas it can be reduced by 50% for the superheated steam at the same temperature range.

Drying Rates

Figure 6 illustrates the drying rates of shrimp in the superheated steam and the hot air at the temperatures of 120 and 140°C. During the early periods of superheated steam and hot air dryings, the drying rates are

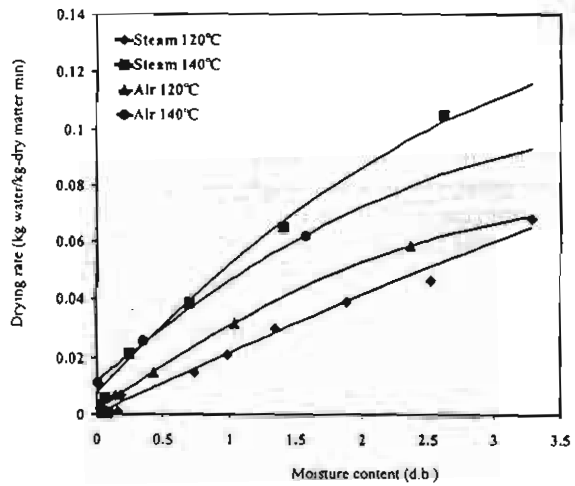

Figure 6. Comparison of drying rates of shrimp in the superheated steam and hot air.

very high due to high water concentration at the surface, thereby allowing the water to be removed easily. In addition, the drying rates decrease almost linearly with the moisture contents. The constant rate period cannot be observed during the drying experiments.

When the temperature of drying media is close to the normal boiling point, the drying rates are relatively lower in the superheated steam than in the hot air. For example, the drying rate in the superheated steam at 120°C is 0.04 kg water/kg dry-matter min at the moisture content of 1.8 d.b. less than twice of that in the hot air under the corresponding conditions. On the other hand, the drying rates in the superheated steam become significantly improved and may be slightly higher than those in the hot air. For example, the drying rates at 140°C for the steam and hot air are respectively 0.07 and 0.06 kg water/kg dry-matter min at the moisture content of 1.4 d.b. According to these results, they indicate the more potential capability of removing the water with the superheated steam at higher temperatures.

Effective Diffusion Coefficients

To determine the effect of temperature on D_{eff}, the experimental shows the relationships of effective diffusion coefficient and temperature for the superheated steam and hot air. The effective diffusion coefficients obtained experimentally for the superheated steam and the hot air as shown in Table 2 were fitted with Eq. (9). These equations are given by

$$\text{Superheated Steam} \quad D_{eff} = 0.00253\exp\left(-\frac{32714.9}{RT_{abs}}\right) \quad R^2 = 0.97 \tag{10}$$

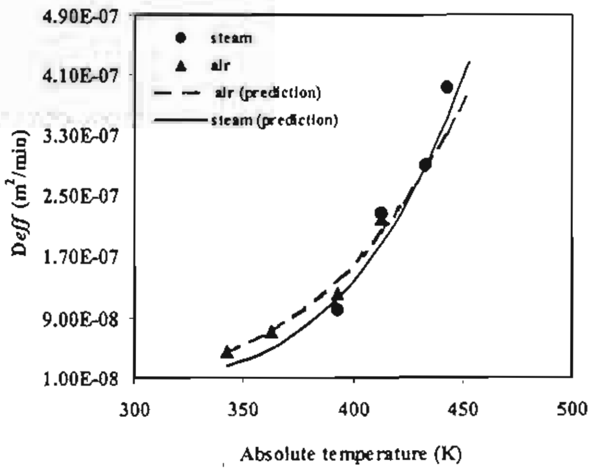

Figure 7. Experimental and calculated values of effective diffusion coefficient.

Table 2. Diffusion Coefficients and Summation of Square Error of Each Test

	Superheated Steam		Air	
Temperature (°C)	D_{eff} (m^2/min)	SSE (d.b.)	D_{eff} (m^2/min)	SSE (d.b.)
70	Nil	Nil	4.53×10^{-8}	1.39
90	Nil	Nil	7.12×10^{-8}	0.53
120	9.93×10^{-8}	0.866	1.22×10^{-7}	0.243
140	2.25×10^{-7}	0.698	2.19×10^{-7}	0.545
160	2.89×10^{-7}	0.197	Nil	Nil
180	3.93×10^{-7}	0.239	Nil	Nil

$$\text{Hot air} \quad D_{eff} = 0.00034\exp\left(-\frac{25578.0}{RT_{abs}}\right) \quad R^2 = 0.99 \tag{11}$$

The results show that the Arrhenius equation is suitably fitted the experimentally determined effective diffusivities for both drying mediums. As indicated in Figure 7, the higher the temperatures the higher the values of effective diffusion coefficient. The effective diffusion coefficient has a higher value for drying in the superheated steam than that in the hot air at above temperature 150°C, resulting in faster drying rate. In contrast, the effective diffusion coefficient in the superheated steam becomes relatively lower at temperature below 140°C. This implies that there exists the inversion temperature between 140 and 150°C for shrimp drying. The reasons for higher effective diffusion coefficient are probably due to the higher convective heat transfer coefficient, thermal conductivity and heat capacity of steam (Mujumdar, 1992; Schwartze and Bröcker, 2000).

The comparison of moisture content in superheated steam and hot air using the effective diffusion coefficients from Eqs. (10) and (11), along with Eq. (8), is shown in Figure 8. It indicates that the superheated steam drying has a more powerful potential for reducing the moisture content at temperature higher than 160°C, comparing to the hot air.

Shrinkage

The shrinkage that occurs during drying process is mainly caused by the water removal. Different drying technique may provide different degrees of shrinkage. Table 3 shows the shrinkage of the dried shrimp products from the superheated steam and hot air at different temperatures. The degree of shrinkage was found to be higher with the increase in temperature. The hot air has a more severe effect on the shrimp shrinkage than the superheated steam under the same temperature.

Colours

Table 4 represents the colours and lightness of the dried shrimp obtained from the superheated steam drying and the local markets. The "L" of the dried shrimp samples in the superheated steam are slightly lower comparing to the local markets whilst the values of "a" and "b" become higher. It can be concluded that the colours of the dried shrimp samples appear slightly more intense yellow and red in the superheated steam drying than in the commercial products. When considered the net

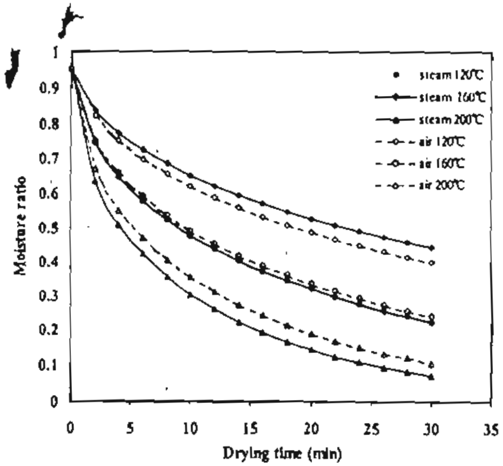

Figure 8. Sensitivity analysis of the fitted effective diffusivities on moisture content at different temperatures.

Table 3. Percentage of Shrimp Shrinkage Dried in Superheated Steam and Hot Air at Different Temperatures

Samples	Shrinkage (%)
Superheated steam at 120°C	13.22 ± 0.08
Superheated steam at 140°C	14.63 ± 0.09
Superheated steam at 160°C	17.22 ± 0.08
Hot air at 120°C	16.02 ± 0.06
Hot air at 140°C	22.81 ± 0.08

Table 4. Values of "a," "b" and "L" for the Dried Shrimp Samples

	Colours			
Samples	L	a	b	ΔE
Superheated steam at 120°C	41.93	6.97	14.85	19.6
Superheated steam at 140°C	42.32	6.07	14.57	19.3
Superheated steam at 160°C	41.00	6.06	15.02	19.1
Local market No. 1	42.87	5.67	13.53	18.6

change in the product colour, the results do not show a remarkable difference for samples dried at 120, 140 and 160°C. The values of the net colour change for those samples have slightly higher than those from the commercial ones. The initial values of a, b and L at the beginning of the experiment are −0.33, −1.13 and 33.14, respectively.

CONCLUSIONS

Desorption isotherms and drying characteristics for shrimps in superheated steam and hot air have been established. The experimental results can be concluded as follows:

1) The GAB model can be used to describe satisfactorily the desorption isotherms of shrimp over a wide range of relative humidity and temperature.

2) Drying rates of shrimp in the superheated steam and the hot air are controlled by the internal diffusion. Drying temperature has a stronger impact on the drying rate and effective diffusion coefficient in the superheated steam than in the hot air.

3) Inversion temperature for drying this material exists between 140 and 150°C.

4) The dried shrimp has a lower degree of shrinkage for drying in the superheated steam than in the hot air.

5) The dried shrimp using the superheated steam at temperatures between 120 and 160°C provides the slight differences of a, b and L as compared to the commercial product.

ACKNOWLEDGMENT

The authors would like to express their sincere thanks to the Thailand Research Fund for financial support.

REFERENCES

Anon. *Official and Tentative* [illegible]

Akao, T. Applications of Pressurized Superheated Steam to Food Processing. In *Chemical Engineering Symposium Series 1*, Shimizui, S., Ed.; Tokyo, Japan, 1983; 239–240.

Blasco, R.; Alvarez, P.I. Flash Drying of Fish Meals with Superheated Steam: Isothermal Process. Drying Technology **1995**, *17*(4&5), 775–790.

Chen, Z.; Wu, W.; Agarwal, P.K. Steam-Drying of Coal. Part 1. Modelling the Behaviour of a Single Particle. Fuel **2000**, *79*, 961–973.

Crawford, D.L. *Meat Yield and Shell Removal Functions of Shrimp Processing*, Special Report 597, Oregon University, Extension Marine Advisory Program. Seafood Laboratory, Astoria, OR. 1981; 6.

Hirose, Y.; Hazama, H. *A Suggested System for Making Fuel from Sewage Sludge*. Kagaku Kogaku Ronbunshu **1983**, *9*, 583–586.

Iglesias, H.A.; Chirife, J. An Alternative to the GAB Model for the Mathematical Description of Moisture Sorption Isotherms of Foods. Food Research International **1995**, *28*, 317–321.

Kechaou, N.; Maalej, M. Desorption Isotherms of Imported Banana Application of The GAB Theory. Drying Technology **1999**, *17*(6), 1201–1213.

Lopez, A.; Iguaz, A.; Eznoz, A.; Virseda, P. Modeling of Sorption Isotherms of Dried Vegetable Wastes From Wholesale Market. Drying Technology **2000**, *18*(4&5), 984–994.

Mujumdar, A.S. Superheated Steam Drying of Paper: Principles, Status and Potential. In *Drying Solids*, Mujumdar, A.S., Ed.; International Science Publisher: New York, 1992; 208–220.

Posomboon, W. Processing Effect on Quality of Dried Shrimp, Master Thesis, Asian Institute of Technology, Bangkok, Thailand, 1998.

Price, R.J. Shrimp, Dried Generic HACCP Plane, http://www.seafood.ucdavis.edu/haccp/plans/shrimp-d.html

Salin, J.G. Steam Drying of Wood for Improved Particle Board and Lower Energy Consumption. Paper and Timber **1988**, *9*, 806–810.

Schwartze, J.P.; Bröcker, S. A Theoretical Explanation for the Inversion Temperature, Proceedings of the 12th International Drying Symposium, Paper No. 93, 2000; 1–10.

Stubbing, T.J. Airless Drying-Developments Since IDS 94. Drying Technology **1999**, *17*(7&8), 1639–1651.

Tarnawski, W.Z.; Mitera, J.; Borowski, P.; Klepaczka, A. Energy Analysis on Use of Air and Superheated Steam as Drying Media. Drying Technology **1996**; *14*(7&8), 1733–1749.

Vázquez, G.; Chenlo, F.; Moreira, R. Modeling of Desorption Isotherms of Chestnut: Influence of Temperature and Evaluation of Isosteric Heats. Drying Technology **2001**, 1189–1200.

Energy optimisation of whole longan drying: simulation results

A. Achariyaviriya*, J. Tiansuwan** and S. Soponronnarit***

SYNOPSIS

The objective of this work is to determine the optimal operating conditions for the process of longan drying. The evaluation criteria of the process are the specific energy consumption and the drying time. Mathematical models were developed to simulate the longan drying process. The models are verified by comparison between the predicted results and experimental measurements. Comparisons between the predicted results and the measurements showed good agreement. The models were used to evaluate the effects of the operating parameters on the specific energy consumption. The operating parameters are drying air temperature, specific airflow rate, and the fraction of recycled air. At the optimal operating conditions, the specific energy consumption was determined to be 4.2 MJ/kg-water.

INTRODUCTION

The longan is an important fruit that grows in Northern Thailand. The production volume of fresh longan fruits fluctuates from season to season depending on climatic conditions and production area. The problem that challenges the longan growers is the overwhelming quantity of longan during the harvest time. The longan drying process can extend the period of time that the fruit can be preserved and can reduce losses arising from seasonal glut. Conventional hot air dryers are widely used to produce longan. In the literature, there are only a few reports on longan drying. Vongnichakul and Phanvuch [1] evaluated the drying constant and sorption isotherms of longan drying. Sitthipranee [2] suggested that the drying air temperature for longan fruit drying using a hot air dryer should be 75°C. Sitthipong *et al.* [3, 4] tested and modified existing dryers of longans by experiments.

Longan drying is an energy intensive process. The energy cost becomes an important factor contributing to the financial success of longan growers. Therefore, studies of the operating parameters of longan drying are necessary in order to determine the optimum drying method to save energy and time. The goals of this work are to develop and simulate a mathematical model of whole longan drying. The effects of drying air temperature and specific airflow rate on specific energy consumption (SEC) are investigated. Also, the effects of dryers with or without air recycling are investigated. To achieve these objectives, drying kinetic equations are developed based on Fick's law, with a homogenous sphere form. Four alternative diffusion models are developed, by modifying the parameters in the Arrhenius equation as a function of moisture content. Desorption isotherms are also developed by fitting the experimental data to the various well-known models.

* Dr Aree Achariyaviriya, Mechanical Engineering Department, Faculty of Engineering, Chiangmai University, Chiangmai, 50200, Thailand.
** Dr Jirawan Tiansuwan, School of Energy and Materials, King Mongkut's University of Technology Thonburi, Suksawat 48 Road, Thungkru, Bangkok, 10140, Thailand.
*** Dr Somchart Soponronnarit, Professor, School of Energy and Materials, King Mongkut's University of Technology Thonburi, Suksawat 48 Road, Thungkru, Bangkok, 10140, Thailand.

MATERIALS AND METHODS

Experimental procedure. In this study, fresh longan fruit of variety E-dor were purchased from the local market. The initial moisture content of whole longan varied from 200 to 260% dry-basis. The uniform sizes of whole longan (average size 25±2 mm in diameter) were selected by measurement with vernier.

Equilibrium moisture contents of whole longan were determined by the static method, using saturated salt solutions. A series of seven different salt solutions (LiCl, $MgCl.6H_2O$, $Mg(NO_3)_2$, NaCl, $(NH_4)_2SO_4$, KNO_3 and K_2SO_4) were used to maintain the relative humidity in a closed container. The experiments were done in a temperature-controlled oven at 45°C, 60°C, 75°C and 85°C.

Volume change or shrinkage of whole longan during drying was studied. The diameter of each fruit was measured by vernier before drying. After drying, with a final moisture content of about 18 % dry-basis, the volume was determined by a liquid displacement technique using toluene at room temperature. A total of 60 duplicate experiments were done under convective drying air of 75°C and drying air velocity of 1 m/s.

The drying experiments were performed in a laboratory hot air dryer with no air recirculation. The experiments were carried out using air temperatures of 52°C, 60°C, 72°C and 82°C with a constant air velocity of 1 m/s. The humidity ratios of the drying air varied from 0.017 to 0.019 kg-water/kg-dry air. In each experiment, the weight of the product was recorded as a function of drying time. Before drying, the diameters of the sample were measured by vernier. Drying was continued until the final moisture content of about 18% dry-basis was reached. Each experiment was replicated three times. The bone-dry moisture contents were determined by using a hot air oven at 103°C for 72 hours.

The rehydration ratio (RR) was defined as the ratio of the mass of the rehydration sample to the dried mass sample. It was determined by soaking the dried sample in distilled water at 30°C for 4 hours [5].

The colour of the dried products was measured using a Spectro-Colorimeter (JUKI JP-7000 Series) and expressed as L (Lightness), a (redness-greenness), and b (yellowness-blueness) values. Each Sample was scanned at three different locations to determine the average L, a and b values. An analysis of variance was used to determine the statistically significant difference ($P<$ 0.05).

Development of desorption isotherms. In this study, the moisture equilibrium models of Brunaruers *et al.* [6], Oswin [7] and Henderson [8] were developed. The parameters were evaluated by fitting the moisture equilibrium experimental data to each moisture equilibrium model using the least square method.

Development of drying kinetic equation. The mathematical model of the drying kinetic equation uses Fick's law of diffusion, where the effective diffusion coefficient depends on moisture content. The whole longan changes its size only slightly during drying; less than 5%. Therefore the effect of product shrinkage during drying is neglected in the analysis. To obtain a solution, a numerical method was used for the analysis with the assumptions that the sample is a homogenous spherical form and the initial moisture content is uniform.

In solving this problem, a solid sphere of radius R is divided into N (N = 50) spherical shells of constant thickness Δr. The spherical shell of radius r is defined by integer j (see Figure 1). It can be written as:

$$r = j\Delta r \qquad \text{for } j = 0, 1, 2, \ldots, N \tag{1}$$

$$R = N\Delta r \tag{2}$$

The mass balance during the increment of time Δt is calculated by taking into account the diffusion of moisture through the surface of radii $(j - 0.5)\Delta r$ and $(j + 0.5)\Delta r$ (shaded area in Figure 1). The new moisture content at position j after time Δt is thus expressed in terms of the previous moisture at the same place and adjacent positions. The equation can be written as:

$$MR_{j,t+\Delta t} = MR_{j,t} + \frac{\Delta t D}{(j\Delta r)^2}\left[(j+0.5)^2 (MR_{j+1,t} - MR_{j,t}) - (j-0.5)^2 (MR_{j,t} - MR_{j-1,t}) \right] \tag{3}$$

The boundary conditions can be written by considering the diffusion of moisture through the surface of the small sphere at the centre (j = 0).

$$MR_{0,t+\Delta t} = MR_{0,t} + \frac{6D\Delta t}{(\Delta r)^2}\left[(MR_{0,t} - MR_{1,t}) \right] \tag{4}$$

The boundary condition at the surface (j = N) can be written as:

$$MR_{N,t} = 0 \tag{5}$$

The initial condition can be written as:

$$MR_{j,0} = 1 \qquad \text{for } j = 0, 1, 2, \ldots, N \tag{6}$$

Development of diffusion models. The effective diffusion coefficient of whole longan was determined by fitting the experimental data to the drying kinetic equation using the least squares method. A Fortran computer program was written to solve the set of equations and it calculated the

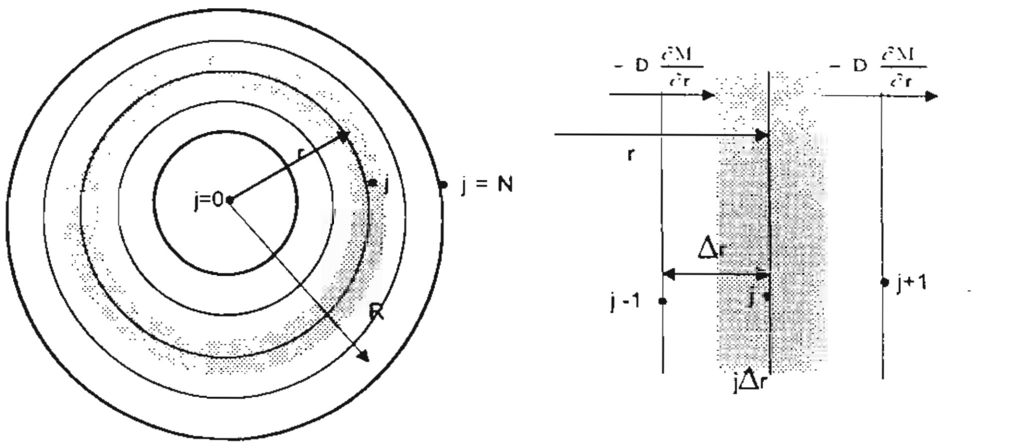

Figure 1 Scheme for a solid sphere, with integer j and for spherical shell of radius r.

moisture distribution inside the solid sphere and the average moisture content as well as the effective diffusion coefficient. To develop the diffusion models, the parameters in the diffusion model were evaluated by fitting the calculated data to each diffusion model. In this study, four different models were developed. The detailed models are as follows:

Model 1. The effective diffusion coefficient is determined by regression analysis of the experimental data to Equation (3). The dependence of the effective diffusion coefficient on the drying air temperature is considered as an Arrhenius-type equation. It is written as:

$$D = D_o \exp [- E_a/RT_{abs}] \tag{7}$$

where D_o is an Arrhenius factor, E_a is an energy of activity, R is the universal gas constant and T_{abs} is the absolute temperature.

Model 2. The effective diffusion coefficient is calculated by fitting the experimental data to Equation (3) at each short time interval, thus obtaining the effective diffusion coefficient as a function of average moisture content in that interval. The dependence of the effective diffusion coefficient on drying air temperature and product moisture content is described by Equation (8). The Arrhenius factor is modified as a second-degree polynomial function of product moisture content. It is written as:

$$D = (a_1 M^2 + a_2 M + a_3) \exp [- E_a/RT_{abs}] \tag{8}$$

Model 3. This model is similar to Model 2. The Arrhenius factor and the energy of activity are modified as a linear function of product moisture content. It is written as:

$$D = (b_1 + b_2 M) \exp [- (b_3 + b_4 M)/RT_{abs}] \tag{9}$$

Model 4. This model is also similar to Model 2. The Arrhenius factor is modified as an exponential function of product moisture content and the energy of activity is modified as a linear function of product moisture content. It is written as:

$$D = [c_1 \exp (c_2 M)] \exp [- (c_3 + c_4 M)/RT_{abs}] \tag{10}$$

Development of a mathematical model. A mathematical model to predict drying performance has been developed for studying the effect of drying air temperature, specific air flow rate and fraction of air recycled on energy consumption.

Calculation of moisture content after drying. The procedures for calculating the moisture content, after drying, of each thin section are: to calculate the effective diffusion coefficient using Model 4; to calculate the equilibrium moisture content using the Oswin model; to calculate the average moisture ratios (MR_f) after drying by integrating $MR_{j,t+\Delta t}$ in Equation (3) over the range j = 0 to N; and then to calculate the moisture content after drying with the following equation.

$$M_f = M_i + (M_{in} - M_{eq})MR_f \tag{11}$$

Calculation of drying air properties after drying. The moist air properties at the outlet of the drying chamber can be calculated by using the principle of mass and energy conservation. From mass conservation, the increase of moisture in the air is equal to the decrease of moisture content in the product. It is given by equation (12).

$$\Delta t\, m_d\,(W_{do} - W_{di}) = m_p\,(M_i - M_f) \qquad (12)$$

From energy conservation, it is assumed that the moist air and product are in thermal equilibrium. The equation can be derived from the first law of thermodynamics. It is given by the following equation.

$$C_a T_{di} + W_{di}(h_{fg} + C_v T_{di}) - C_a T_{do} - W_{do}(h_{fg} + C_v T_{do}) = 0 \qquad (13)$$

Calculation of electricity consumption at blower. The rate of electricity consumption (E_{blower}) for driving the blower can be calculated by following equation.

$$E_{blower} = m_d P/(\rho_a e_b e_m) \qquad (14)$$

Calculation of heat consumption at heater. The rate of heat consumption (E_{heater}) can be calculated by following equation.

$$E_{heater} = m_d\,(C_a + C_v W_{di})\,(T_{di} - T_{amb} - T_{blower}) \qquad (15)$$

where T_{blower} is the temperature rise of the drying air across a blower. It can be calculated from an equation derived from the first law of thermodynamics for steady flow. It can be written as:

$$T_{blower} = P/[\rho_a e_b (C_a + C_v W_{di})] \qquad (16)$$

Calculation of specific energy consumption. The specific energy consumption is defined as:

$$SEC = DT^*\,(2.6\,E_{blower} + E_{heater}) / [(M_{in} - M_{fi})\,m_p]$$

where the value of 2.6 is the energy conversion factor.

RESULTS AND DISCUSSION

Desorption isotherm. The Oswin model presents the highest value of coefficient of determination ($R^2 = 0.96$) and the lowest value of mean residual square (MRS = 0.0019). The parameters in the models are shown in Table 1. It was found that the Henderson model is in good agreement with experimental data in the relative humidity range of less than 80%. The model of Brunaruers *et al.* (BET model) does not agree with the experimental data, especially for low relative humidity. Oswin's model agrees very well with experiment in the entire range of relative humidity.

Drying kinetic equations. Experimental results showed that there was no constant drying rate period. Shrinkage of whole longan was negligible because it was lower than five percent. The effective diffusion coefficient is calculated by curve fitting and then the parameters in the diffusion models are calculated by fitting the calculated data to each diffusion model. Figure 2 shows the effective diffusion coefficient as a function of moisture content. It can be seen that the effective diffusion coefficient increases with decreasing moisture content for Models 2, 3 and 4. Generally, the effective diffusion coefficient increases with increasing moisture content. However, it has been reported that the effective diffusion coefficient increases with decreasing moisture content for carrot [9] and corn [10]. The results are shown in Table 2. It can be seen from Table 2 that Model 3 gives the minimum value of MRS.

Quality of dried product. Table 3 shows the lightness (L), redness (a), yellowness (b), and rehydration ratio (RR) values of the dried whole longan's aril which are significantly affected by drying air temperatures in the analysis of variance. It can be seen that the RR and a-values increased with drying air temperatures but the L-value and

Table 1 Equilibrium moisture content models of whole longan.

Name of model	Type	* R^2	** MRS
Henderson	$1 - RH = \exp[-0.025108 T_{abs} M_{eq}]^{1.41141}$	0.57	0.0064
BET	$\dfrac{RH}{(1-RH)M_{eq}} = \dfrac{1}{cM_m} + \dfrac{(c-1)}{cM_m} RH$ where $M_m = 13.3415 + 8.4125T$, $c = -0.25684 \exp(-0.001595T)$	0.59	0.0118
Oswin	$M_{eq} = 0.16187[RH/(1-RH)]^{(0.7095 - 0.00386T)}$	0.96	0.0019

$^* R^2 = \sum_{i=1}^{n} [(MR_{pr})_i - (MR_{ex})_{av}]^2 / \sum_{i=1}^{n} [(MR_{ex})_i - (MR_{ex})_{av}]^2$ $\qquad$ $^{**} MRS = \sum_{i=1}^{n} [(MR_{pr})_i - (MR_{ex})_i]^2 / n$

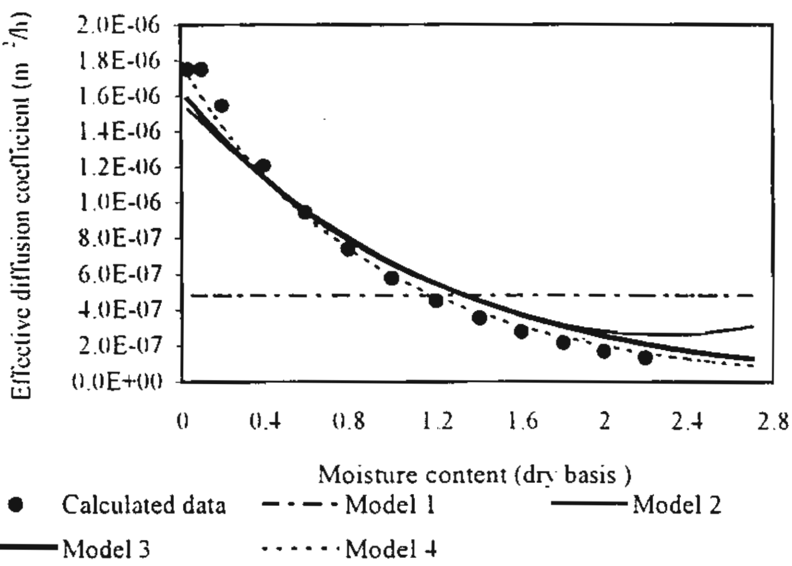

Figure 2
Effective diffusion coefficient of whole longan drying calculated by various models (drying air temperature 60°C).

Table 2 Diffusion models of whole longan drying.

Model	Diffusion model	* R^2	** MRS
Model 1	$D = 122.6786 \exp[-6444.47 / T_{abs}]$	0.65	0.0075
Model 2	$D = (0.00663M^2 - 0.0302M + 0.0412) \exp[-28188 / RT_{abs}]$	0.87	0.0024
Model 3	$D = (0.02343M + 0.0067) \exp[(-26509.2 - 3214.68M) / RT_{abs}]$	0.88	0.0020
Model 4	$D = 0.003375 \exp(4.2916M) \exp[(-20900.8 - 14916.2M) / RT_{abs}]$	0.89	0.0025

* $R^2 = \sum_{i=1}^{n} [(MR_{pr})_i - (MR_{ex})_{av}]^2 / \sum_{i=1}^{n} [(MR_{ex})_i - (MR_{ex})_{av}]^2$ ** $MRS = \sum_{i=1}^{n} [(MR_{pr})_i - (MR_{ex})_i]^2 / n$

b-value decreased. The L-value decreases at high drying air temperature due to browning reactions. There is no significant difference ($P > 0.05$) in RR-values for all pairs of experimental values. At drying air temperature 50°C and 65°C, there are no significant difference ($P > 0.05$) in a, b and RR-values and the products are found to be a brown-red colour. When they are dried with drying air temperatures of 75°C and 85°C; the colours of the samples are found to be brown and black brown, respectively. The brown dried longan is the colour demanded by the market [11].

Table 3 Objective colour and rehydration ratio of dried whole longan.

Temperature	L	a	b	RR
50	23.94	3.71	6.08	2.92
65	22.65	7.92	5.91	3.02
75	20.60	4.16	3.92	2.94
85	18.37	4.97	2.18	2.95

Values followed by the same letter in the same column are not significantly different at $P > 0.05$.

Verification of mathematical model. The evolution of experimental and simulated moisture contents of whole longan are shown in Figure 3. The drying conditions are drying air temperature of 75°C, the diameter between 2.1 and 2.5 cm, specific air flow rate of 338 kg/h-kg dry product, dry mass product of 1.19 kg, initial and final moisture contents of 242 and 17% dry-basis, respectively. It is seen that the simulated moisture contents are lower than experimental results at the beginning of drying but a little bit higher towards the end of drying. The specific energy consumptions obtained from the model and experiments are 228 and 197 MJ/kg of water evaporated, respectively. The drying times are 47 and 40 h, respectively.

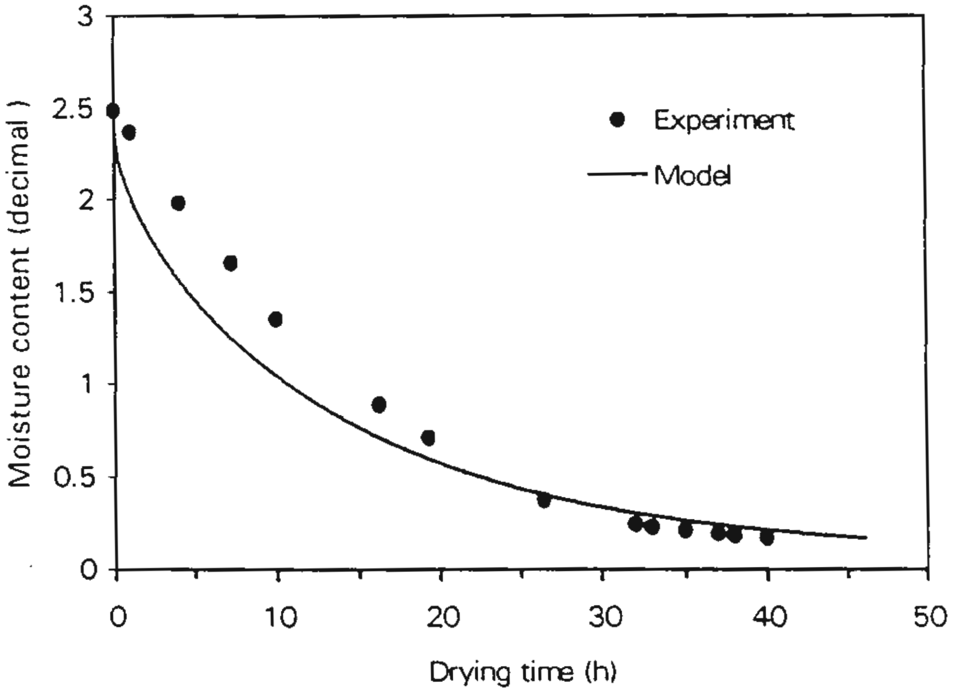

Figure 3
Comparison of simulated and experimental moisture content of whole longan during drying at drying air temperature of 75°C and 0% of recycled air. (The diameter of longan between 2.1 and 2.5 cm, specific air flow rate of 338 kg/h-kg dry product, dry mass product of 1.19 kg, initial and final moisture contents of 242 and 17% dry-basis, respectively).

Effect of specific air flow rate. Figure 4 shows the effect of specific air flow rate (SAF) on specific energy consumption and drying time at a drying air temperature of 70°C. The simulated drying conditions are SAF varying from 14 to 30 kg-dry air/h-kg dry longans, fraction of air recycled (RC) of 0% initial longan-weight of 1000 kg, ambient temperature of 35°C, ambient humidity ratio of 0.015 kg-water/kg-dry air, and initial and final moisture content of 316% and 18% dry-basis, respectively. It is found that the SEC depends upon the SAF, i.e. the SEC decreases with

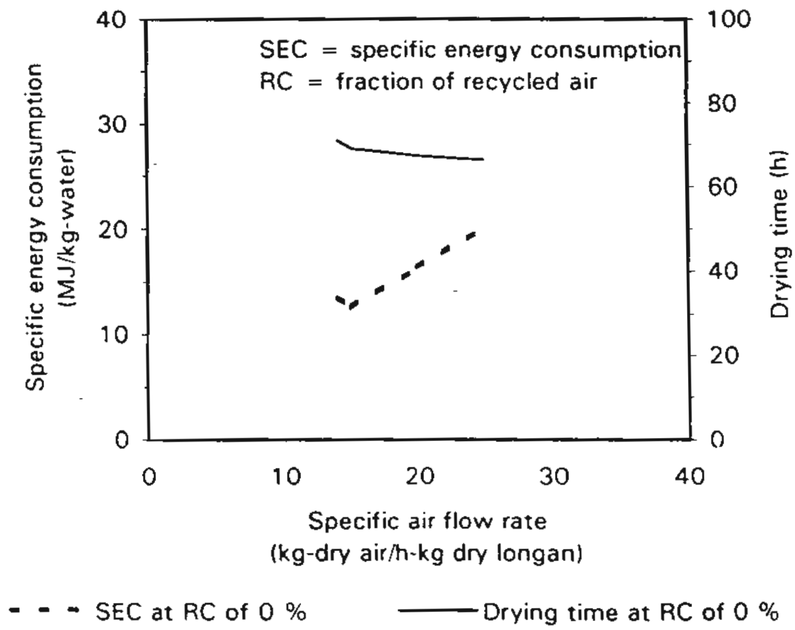

Figure 4
Effect of specific air flow rate on specific energy consumption with no recycled air. (Initial longan-weight of 1,000 kg, initial moisture content of 316% dry-basis, final moisture content of 18% dry-basis, ambient temperature of 35°C, ambient humidity ratio of 0.015 kg water/kg dry air and drying air temperature of 70°C.)

increasing SAF to a minimum point, and then increases due to an excessive air flow rate. It is also found that the drying time (DT) depends upon the SAF, i.e. the DT decreases rapidly with increasing SAF when the SAF is small, but thereafter the DT is nearly constant.

Effect of drying air temperature. The effect of drying air temperature on SEC was also studied. Figure 5 shows SEC and DT versus drying air temperature. The simulated drying conditions are drying air temperature varying from 65 to 90°C, RC of 0%, and SAF of 25 kg-dry air/h-kg dry longans. Other conditions are the same values as the previous conditions. It is found that the drying air temperature affects both SEC and DT, i.e. the SEC decreases a little bit with increasing drying air temperature, but the DT decreases markedly with increasing drying air temperature.

Effect of fraction of air recycled. Figure 6 shows the effect of the fraction of air recycled (RC) on the SEC and drying time at various drying air temperatures. The simulated drying conditions are RC varying from 0 to 95%, SAF of 25 kg-dry air/h kg-dry longans and drying air temperatures of 65, 75 and 85°C. Other conditions are the same values as the previous conditions. It is found that the SEC decreases with increasing RC to a minimum value, and then the SEC increases since humidity ratio in the drying air is an over high value. Consequently, the drying time increases. The optimum SEC of 4.2 MJ/kg-water occurs at RC of 90%, SAF of 25 kg-dry air/h-kg dry longans, drying air temperature of 75°C and drying time of 56 hours.

CONCLUSIONS

Mathematical models have been developed to simulate the longan drying process. The diffusion model, using the activation energy as a linear function of moisture content and the Arrhenius factor as an exponential function of moisture content, together with Oswinís moisture equilibrium model, predicted the best results, as compared to the experimental measurements.

The whole longan drying process was simulated with the models. The optimal operating conditions were determined when the drying air temperature is 75°C, the fraction of recycled air is 90%, and the specific air flow rate is 25 kg-dry air/h-kg dry longan. The specific energy consumption at the optimal conditions is predicted to be 4.2 MJ/kg-water, and the dry time is 56 hours. The shrinkage of whole longan after drying is less than 5% at this temperature. This result shows a drastic reduction of the specific energy consumption, as a non-optimised drying process may require as much as 20 MJ/kg-water.

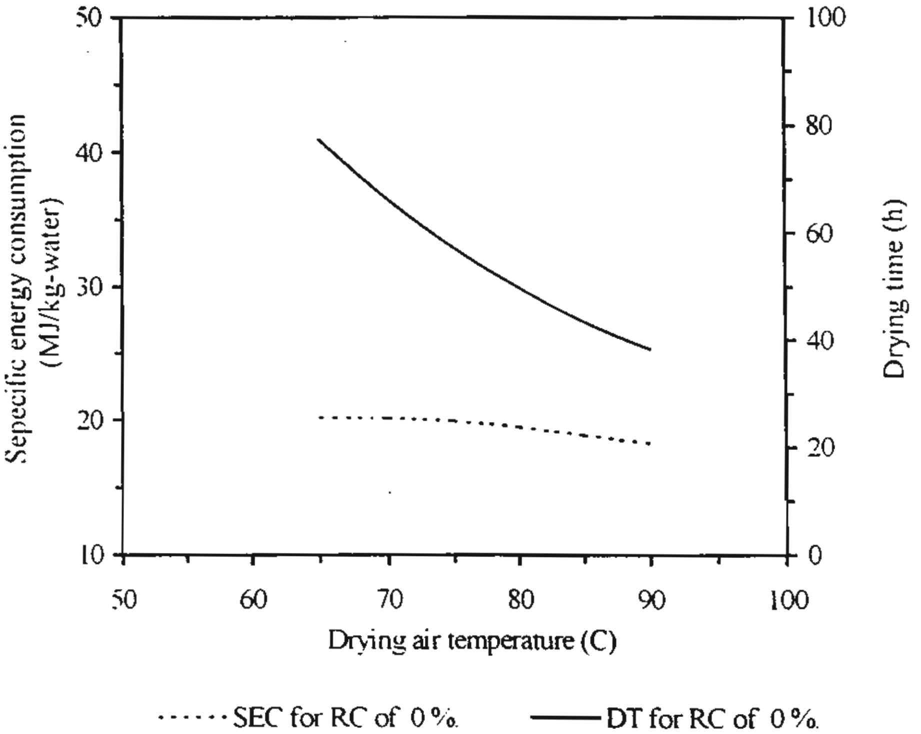

Figure 5
Effect of drying air temperature on specific energy consumption with no recycled air. (Initial longan-weight of 1,000 kg, initial moisture content of 316% dry-basis, final moisture content of 18% dry-basis, ambient temperature of 35°C, ambient humidity ratio of 0.015 kg water/kg dry air.)

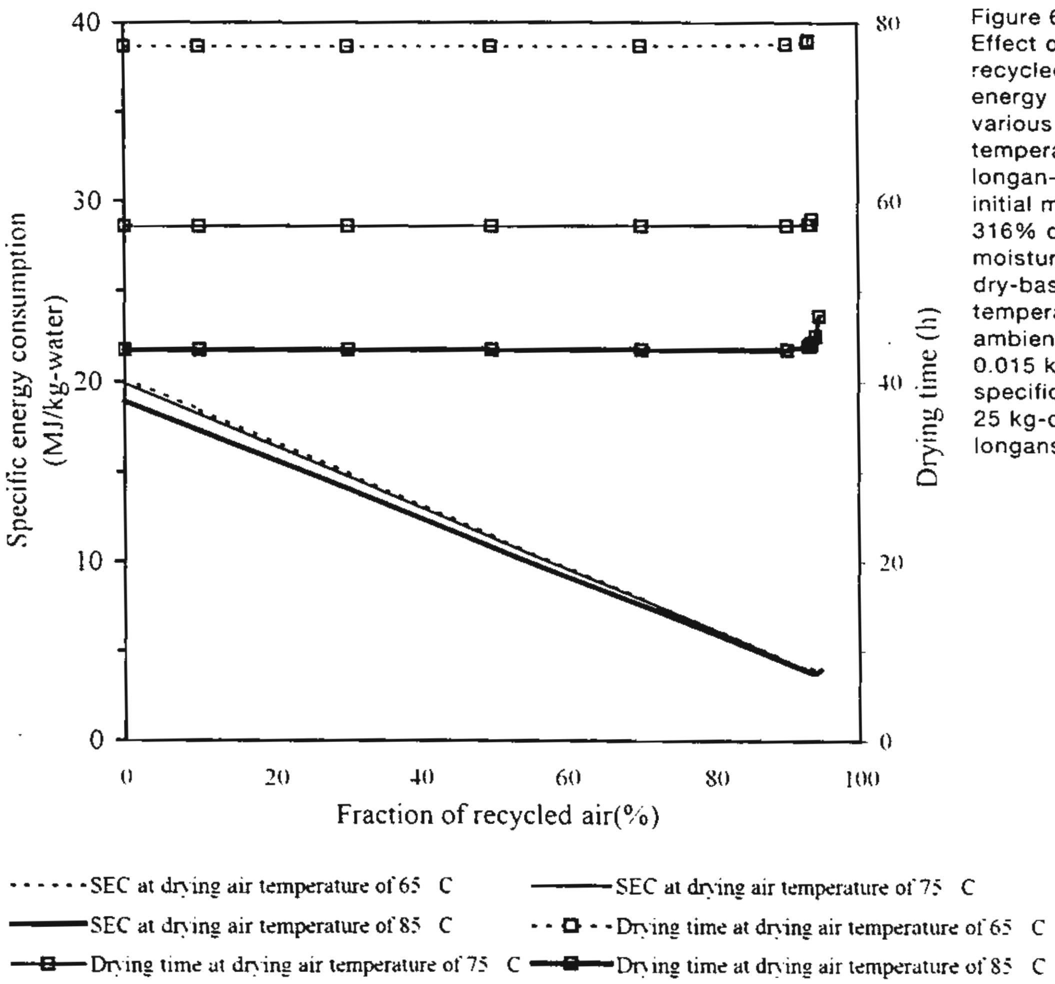

Figure 6
Effect of fraction of recycled air on specific energy consumption at various drying air temperatures. (Initial longan-weight of 1,000 kg, initial moisture content of 316% dry-basis, final moisture content of 18% dry-basis, ambient temperature of 35°C, ambient humidity ratio of 0.015 kg water/kg dry air, specific air flow rate of 25 kg-dry air/h-kg dry longans.)

NOMENCLATURE

a redness
a_1, a_2, a_3 constants in Equation (8)
b yellowness
b_1, b_2, b_3, b_4 constants in Equation (9)
C specific heat capacity, kJ/kg-°C
c_1, c_2, c_3, c_4 constants in Equation (10)
D effective diffusion coefficient, m²/h
D_o Arrhenius factor, m²/h
DT drying time, h
E the rate of electricity consumption, kJ/h
E_a energy of activity, kJ/mole
e_b efficiency of blower
e_m efficiency of motor
h_{fg} specific evaporated enthalpy, kJ/kg
L lightness
M moisture content , decimal dry-basis
m_p dry mass of product, kg-dry longans
m_d mass flow rate of dry air, kg-dry air/h
MR moisture ratio, decimal
R universal gas constant, kJ/mole-K
RC fraction of air recycled, %
RH relative humidity, decimal
RR rehydration ratio
SAF specific airflow rate, kg-dry air/h-kg dry longans
SEC specific energy consumption, MJ/kg-water
t drying time , h
Δt time interval, h
T temperature, °C
W humidity ratio , kg-water/kg-dry air
ρ density, kg/m³

Subscripts

a air
amb ambient condition
di entering drying chamber
do leaving drying chamber
eq equilibrium condition
ex experimental value
f after drying
fan after blower
i before drying
in initial condition

mix after mixing
n the number of observations
pr predicted value
v vapour

ACKNOWLEDGEMENTS
The authors would like to express their sincere thanks to the Thailand Research Fund for the financial support of this research.

REFERENCES

1. Vongnichakul, R. and R. Phanvuch. "Study of Equilibrium Moisture Content and Drying Constant of Longan". Master of Engineering Thesis, Department of Mechanical Engineering, Chiang Mai University, 1997.
2. Sitthipranee, P. "Longan Drying". Industry Journal, Vol. 33, No. 8, 1990, pp. 36–39.
3. Sitthipong, N., Hirun, A., Klongpanich, W., Thertoon, P., Siratanapanta, T., Thavornun, S. and Kamalaspitak, S. Multi-crop Dryers Project. Final report (Phase 1), IDRC File No. 3-P-88-0234. Department of Mechanical Engineering, Chiang Mai University. 1988.
4. Sitthipong, N., Hirun, A., Siripabpra, P., Rerkkriangkrai, P., Achariyaviriya, S., Thavornun, S. Promwungkwa, A. and Kamalaspitak, S. Multi-crop Dryers Project. Final report (Phase 2), IDRC File No. 3-P-88-0234. Department of Mechanical Engineering, Chiang Mai University. 1992.
5. Gabas, A. L., Menegalli, F. C. and Telis-Romero, J. "Effect of chemical pretreatment on the physical properties of dehydrated grapes". Drying Technology, Vol. 17, No. 6, 1999, pp. 1215–1226.
6. Brunaruers, S., Emmett, P. H. and Teller, E. "Adsorption of gases in multimolecular layers". Journal of American Chemical Society, Vol. 6, 1938, pp. 309–319.
7. Oswin, C. R. "The kinetics of package life III". The isotherm. Journal of Chemical Industry (London), Vol. 64, 1946, pp. 479–421.
8. Henderson, S. M. "A basic concept of equilibrium moisture". Agricultural Engineering, Vol. 33, 1952, pp. 29–31.
9. Kompany, E., Benchimol, J., Allaf, K., Ainseba, B. and Bouvier, J.M. "Dehydration kinetics and modeling". Drying Technology, Vol. 11, 1993, pp. 451–470.
10. Ulku, S. and Uckan, G. "Corn drying in fluidize beds". Drying '98, Vol. 2, 1986, pp. 531–536.
11. Attabhanyo, R., Menuam, L. and Wongsawadi, S. "A study on different methods of dehydration suitable for each variety of longana". Faculty of Agriculture, Chiang-Mai University, unpublished paper, 1977.

The International Journal of Ambient Energy

Volume 23, Number 4 October 2002

Editor
M W Liddament

Co-ordinating Editor
A F C Sherratt

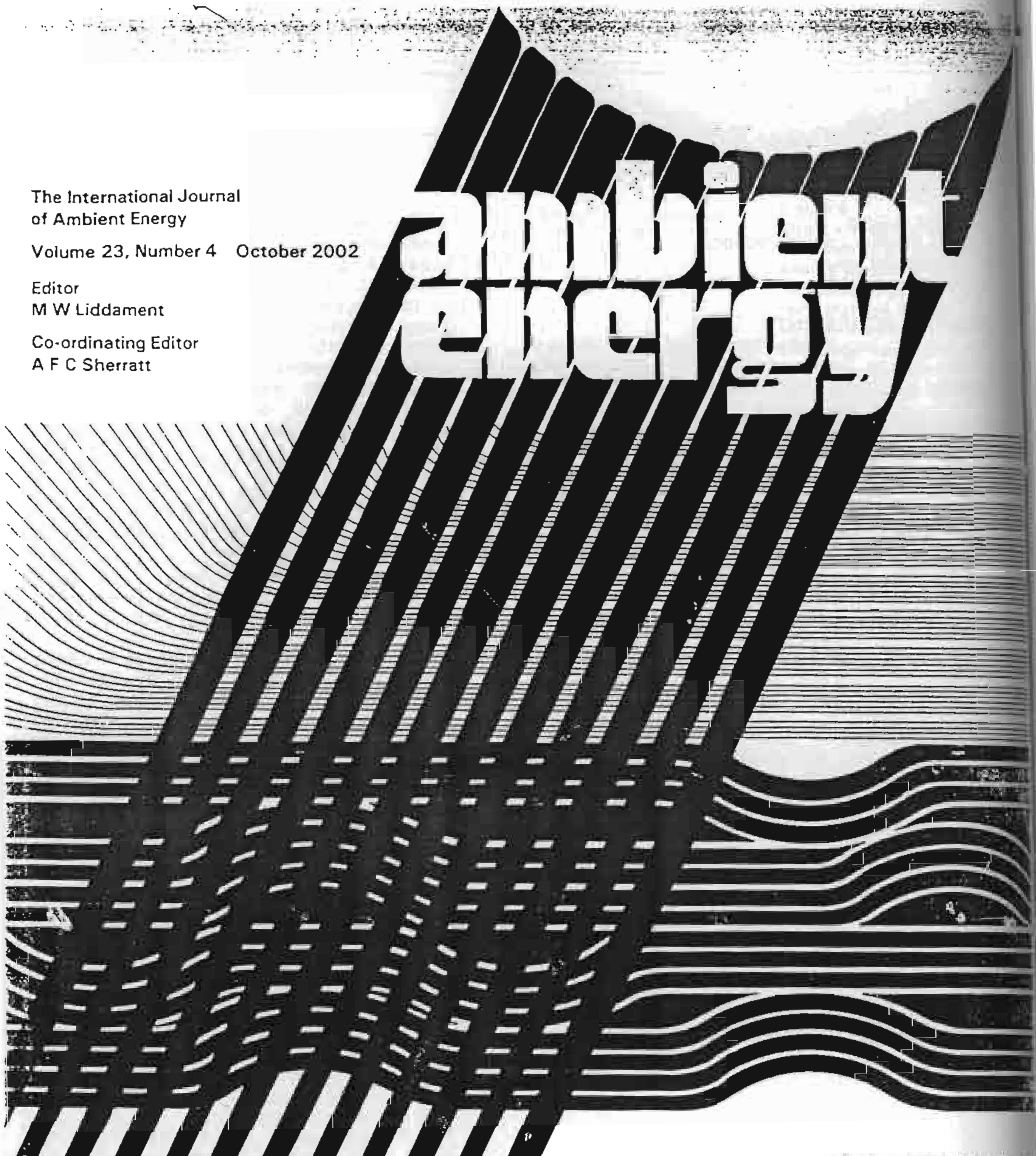

ELSEVIER

Journal of Food Engineering 58 (2003) 67–73

JOURNAL OF FOOD ENGINEERING

www.elsevier.com/locate/jfoodeng

Superheated steam fluidised bed paddy drying

Chaiyong Taechapairoj [a,*], Isares Dhuchakallaya [a], Somchart Soponronnarit [a], Somboon Wetchacama [a], Somkiat Prachayawarakorn [b]

[a] Thermal Technology Division, School of Energy and Materials, King Mongkut's University of Technology Thonburi, Suksawat 48 Road, Thungkaru, Bangkok 10140, Thailand

[b] Faculty of Engineering, King Mongkut's University of Technology Thonburi, Suksawat 48 Road, Thungkaru, Bangkok 10140, Thailand

Received 18 February 2002; accepted 24 July 2002

Abstract

Fluidised bed paddy drying using superheated steam is a newly alternative approach instead of using the conventional hot air. The mechanism of mass transfer for paddy drying in a range of initial moisture content between 25% and 44.5% d.b. is strongly controlled by internal moisture movement inside the kernel and a two-series exponential equation is suitably used to explain its movement. Drying parameters in the equation are a function of temperature and bed depth. For the paddy quality, head rice yield from the superheated steam drying is more sustainable and has higher values than those obtained from the hot air drying, whereas the colour of white rice becomes darker, making it poorer quality. The percentage of white belly is significantly affected by the initial moisture content.

Keywords: Dehydration; Grain; Head rice; Quality; Superheated steam; White belly

1. Introduction

Paddy is an important food crop in the world. This cereal is processed into several products, in addition to a staple food. Before being processed, freshly-harvested paddy needs to be dried in order to avoid the quality deterioration by microorganisms and respiration.

A drying method which is utilised effectively for essentially high moisture grains, for example, paddy, parboiled rice, soybean and maize, is a fluidisation technique, in which air and solid particles are rigorously mixed. It has been suggested that high moisture paddy should be dried quickly to approximate 23% d.b. to prevent the yellowing of rice kernels which is easily occurred at high moisture level and then subjected to ambient air drying in a storage bin until its moisture content is down to 16% d.b. (Soponronnarit & Prachayawarakorn, 1994). Sutherland and Ghaly (1990) undertook an intensive investigation into the feasibility of using a hot-air fluidised-bed drying technique for paddy. Their experiments showed that the head rice yield related to the final moisture content: the head rice yield was 58–61% when paddy was dried from 28.2% to 20.5% d.b. but was 15–24% for a final moisture content lower than 20% d.b.

The drying medium which is used for carrying the evaporated water and fluidising solid particles could be hot air or superheated steam. Superheated-steam drying offers important advantages over hot air drying: (I) the energy supplied to the dryer can be reduced economically by recycling the exhaust steam in a closed loop, (II) the energy from the exhaust steam resulting from the evaporation of moisture inside the solids can be recovered and used in the other sections, (III) environmental pollution or odour emission to the atmosphere can be eliminated since drying occurs in a closed chamber without air.

The general characteristics of the drying process change significantly when superheated steam is used instead of hot air. The major differences include: (I) steam condensation at the material surface during the initial drying period, (II) higher drying rate in superheated steam than in hot air at above inversion temperature, the temperature at which the evaporation rate of water into steam and hot air becomes equal (Yoshida & Hyodo, 1963), (III) no gas film resistance around the solid surface thereby increasing the mass transfer rate.

*Corresponding author. Tel./fax: +662-470-8663.
E-mail address: chaiyong_t@yahoo.com (C. Taechapairoj).

0260-8774/02/$ - see front matter © 2002 Elsevier Science Ltd. All rights reserved.
PII: S0260-8774(02)00335-7

The use of a high steam temperature may cause a serious problem for thermally sensitive food materials, such as browning, discolouration and protein denaturation. In some cases, however, it changes the textural property beneficially; for example, shrimp drying with superheated steam presented a lower degree of shrinkage than that using hot air (Prachayawarakorn, Soponronnarit, & Jaisut, 2002).

The purpose of the present work was to make the parboiled rice by a superheated-steam fluidised-bed dryer. The drying characteristics of paddy were investigated, along with the qualities in terms of head rice yield, whiteness and white belly to be determined.

2. Material and methods

A batch superheated-steam fluidised-bed dryer is schematically illustrated in Fig. 1. It consisted of five main components: a cylindrical chamber with an inner diameter of 15 cm and a height of 100 cm, a 13.5 kW electrical heater for converting saturated-steam to superheated-steam, a backward-curved blade centrifugal fan driven by a 2.2 kW motor, a reverse flow cyclone

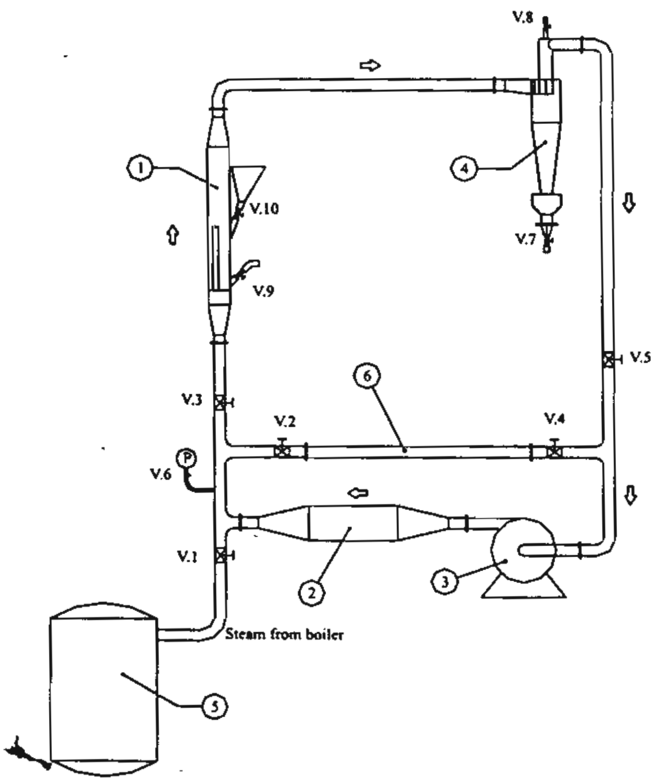

Fig. 1. A schematic diagram of the superheated-steam fluidised bed dryer: (1) fluidised bed dryer, (2) heater, (3) fan, (4) cyclone, (5) boiler and (6) bypass line.

and a small boiler with a 31 kg/h capacity of generating steam. A perforated sheet, with 10 holes per cm^2, was used for distributing the drying medium. The ratio of the diameter of dryer to grain diameter designed was large enough to minimise the wall effect. However, the wall effect becomes important when the ratio is lower than 10 (Geankoplis, 1995). Superheated-steam temperature was controlled by a PID controller with an accuracy of ± 1 °C. Before using steam for drying, hot air was used for warming up the system until the temperature in every part reached the desired level. Then, the air was replaced by steam. The steam generator generated the saturated-steam at 106 kPa (absolute pressure) with the corresponding temperature of 100 °C. When the saturated steam was flowed through the electrical heater, additional heat was supplied to raise the steam temperature up to the desired level. It was subsequently passed through the fluidised-bed dryer. After that, the small dust particles and the immature grains suspended in the exhaust steam were collected in the cyclone. Finally, all the cleaned exhaust steam was reused again.

The paddy was rewetted to a desired moisture content and then kept in a cool room at the temperature of 3–5 °C for 5–7 days to ensure uniform moisture content throughout the kernels. The experimental conditions were set up as follows: initial moisture contents of 25–45% d.b., bed depths of 10–15 cm, superheated steam temperatures of 150–170 °C at a fixed superficial velocity of 3.1 m/s. Temperatures at different positions were measured by Chromel–Alumel thermocouples (Type K) connected to a data logger with an accuracy of ± 1 °C. After drying, paddy kernels were slowly cooled down to ambient temperature and kept in a polypropylene bag. Then, they were gently ventilated with ambient air until their moisture content reached 16% d.b. Finally, a 300 g sample was kept in a seal plastic bag for 2 weeks before testing for head rice yield, whiteness and white belly.

The moisture content of paddy was determined by an electrical air oven at a temperature 103 °C for 72 h, according to AACC method, 1995. Paddy qualities in terms of head rice yield and whiteness were determined quantitatively and compared to the reference sample (paddy dried by the ambient air). The methods followed the guideline of the Ministry of Agricultural and Cooperatives, Thailand. Head rice is defined as milled rice having a kernel length at least 75% of its original length. The head rice yield was defined as the mass of white rice that remains as head rice after complete milling divided by the mass of paddy sample.

From the experiments, the head rice yield of fresh paddy samples obtained each time was different and it was thus difficult to compare the paddy quality obtained from different drying conditions. To make a clear comparison, the head rice quality was therefore represented as a relative head rice yield. The relative head rice yield is defined as the ratio of head rice obtained from artificial drying to that from the natural air drying.

In addition to the head rice yield, the other two qualities of paddy, translucence, which was directly measured by whiteness, and white belly, were also examined. The opaque white spot at the paddy kernel can be loosely divided into the white belly and the chalky grain. The white belly arises from incomplete or partially gelatinised paddy, while the chalky grain has its own characteristic depending upon the genotype of paddy and can still exist in the grain even with complete gelatinisation. The white rice samples were measured for the colour by using a Kett digital whiteness meter (Model C-300). Before measuring the colour of a sample, the whiteness meter must be calibrated with a white coloured reference, having a standard value of 86.3. Throughout this work, the colour of the sample was represented in terms of the relative whiteness, which was defined as the whiteness of the sample from the artificial drying divided by that from natural drying.

3. Results and discussion

3.1. Fluidisation conditions

At first, the minimum velocity required for fluidising in the superheated steam was determined by measuring the pressure drop. The results are shown in Fig. 2 for bed depths of 10, 12.5 and 15 cm, indicating that the minimum superficial velocity for fluidisation (U_{mf}), determined from the point where the pressure drop begins to be constant, is independent on the bed depth with a value of 2.6 m/s for a steam temperature of 150 °C. This minimum velocity is higher than that using hot air for which the velocity was 1.65 m/s as previously reported by Soponronnarit and Prachayawarakorn (1994). The required higher fluidising velocity is probably due to the lower density and viscosity of superheated steam. The lower physical properties of steam result in the ratio

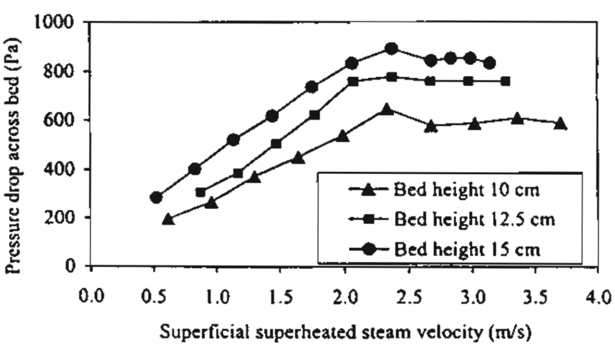

Fig. 2. Relationship between pressure drop and superficial superheated velocity at different bed height (superheated steam temperature = 150 °C).

of the vertical force on the paddy becoming lower for the same superficial velocity. However, the force acting on the paddy kernel in the opposite direction can be offset by increasing the superficial steam velocity, thus requiring a higher minimum fluidising velocity for steam.

As can be seen in Fig. 2, below the minimum fluidising velocity, the bed is a static bed, corresponding to the region where pressure drop has a linear increase with superficial velocity. However, at the onset of fluidisation, the paddy was partially fluidised and it required a velocity at least 1.3 times higher than the minimum superficial fluidising velocity to achieve all particle movement.

When applying the Ergun equation (1952), the calculated minimum fluidisation velocity was 2.30 m/s at a temperature 150 °C, slightly lower than the experimentally determined value. This might be because of the agglomeration of paddy kernels caused by the steam condensation. Fig. 3 shows the minimum fluidising velocity for air and superheated steam, and indicates the slight dependence of fluidising velocity on temperature, but the strong dependence on the characteristic fluid medium, with the higher fluidising velocity for steam over a wide range of temperatures. The small effect of temperature on the fluidising velocity might be because of a small change in the density and viscosity of the mediums for the range of temperature considered. The characteristic properties of paddy used in the calculation of the fluidising velocity are shown in Table 1.

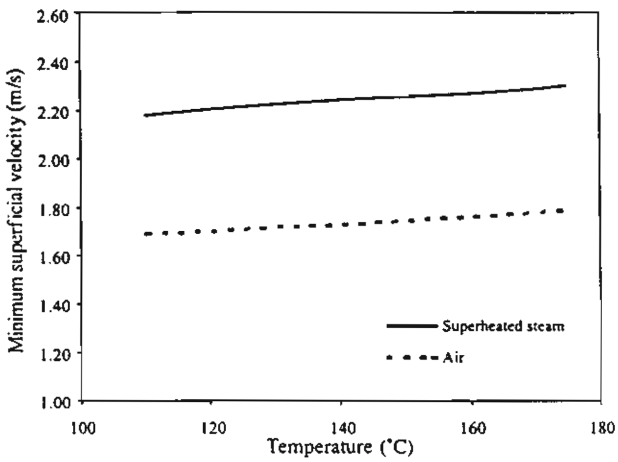

Fig. 3. Effect of drying media on the fluidising velocity.

Table 1
Properties of long grain paddy

Physical properties	
Equivalent diameter (mm)	3.5
True density (kg/m^3)	1414
Void (ε_{mf}) (Soponronnarit & Prachayawarakorn, 1994)	0.557
Sphericity ($\emptyset$)	0.68

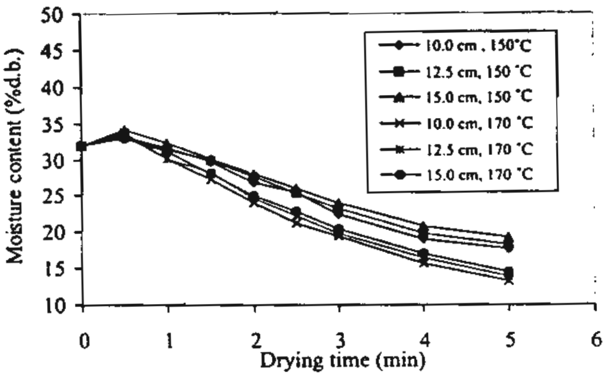

Fig. 4. Variation in moisture content of paddy at different bed heights and inlet superheated steam temperatures.

3.2. Drying behaviour

Fig. 4 shows the behaviour of paddy kernels dried in superheated steam at different temperatures and bed heights. In the first half a minute, the paddy kernels adsorb a small amount of the condensed water and thus, their temperature rapidly increases to the saturation point corresponding to 100 °C. As can be seen in this figure, the samples can gain water evenly although the operating conditions such as temperature and bed depth are changed. Such results are dissimilar to the work reported by Tang and Cenkowski (2000), who studied potato drying in a batch tray dryer using superheated steam. In their work, the initial gain in moisture content varied with the temperature; the samples could gain more moisture at lower steam temperatures. A possible reason for this contradiction can be that using a high steam velocity in the present work (>3 m/s for the fluidised bed) leads to the combination of high heat and mass transfer rates. Thus, the large amount of condensed water existing between the kernels evaporates rapidly, instead of diffusing into the grains. From Fig. 4, the initial gains in moisture content for samples at different conditions are approximately 0.02 d.b.

Fig. 5 represents the comparative drying characteristics of paddy in superheated-steam and hot air. After passing through the condensation stage, the moisture content reduces exponentially with drying time, indicating that the main resistance to moisture movement is in the interior. In this moisture reduction step, the drying curve is very similar to that found in the hot air drying, but the total drying time for steam is shorter in spite of the existence of condensation period. The faster moisture reduction is due to the higher heat transfer rate with superheated-steam at this temperature. The total drying time for obtaining a given moisture content decreases with increase in steam temperature, as expected. This is consistent with the fundamental drying theory, which expects a higher heat transfer flux to the bed of paddy with higher temperature.

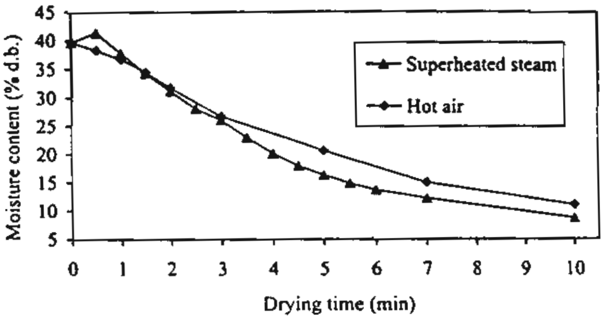

Fig. 5. Comparison of drying rates of paddy dried under superheated steam and hot air drying (temperature = 150 °C, bed height = 10 cm and velocity = $1.3U_{mf}$).

Besides the effect of temperature, the bed depth or, in the other words, the total surface area of grains in the bed is another factor that reflects the amount of water evaporation from the grains; thicker grain bed depths lead to lower moisture reduction rates for a single gain, thereby giving a longer drying time. This is because the heat supply is rather small, along with the poorer heat convection. As previously shown in Fig. 4, it clearly demonstrated that temperature had a greater contribution than bed depth.

3.3. Modified thin-layer drying equation

During the course of drying in the fluidised bed dryer, paddy was suspended in the high steam velocity (except for initial drying period) with constant steam temperature, which fully stratifies the thin layer drying. In such circumstances, the bed should be very thin. However, according to our experiments, the bed depth had an effect on moisture content. Therefore, the thin layer equation is modified, so that the drying constants account for the bed depth, in addition to temperature. The two-series exponential model for thin layer drying of grains has been chosen to correlate the experimental data,

$$MR = \frac{M(t) - M_{eq}}{M_{in} - M_{eq}} = A\exp(-k_1 t) + B\exp(-k_2 t) \qquad (1)$$

where A, k_1, B and k_2 are the drying constants varying with the operating conditions. M_{eq}, M_{in} and $M(t)$ are the equilibrium moisture content and the moisture content at $t = 0$ and t, respectively. In the present work, the steam temperature above the normal boiling point was used, so that it might be reasonable to assume the moisture content at equilibrium to be zero.

A multiple regression technique was used to determine the drying constants. To get a more accurate result, the possible correlation equations between the drying constants and the operating conditions were substituted into Eq. (1) and then statistically fitted with

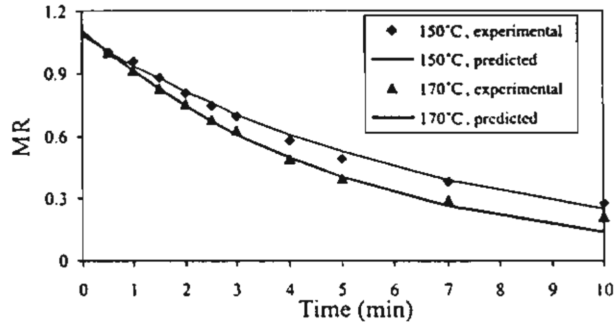

Fig. 6. Experimental data and the predicted drying curve under superheated steam (bed height 10 cm and velocity = $1.3U_{mf}$).

all the data from the whole set of experimental conditions, except for that data from the condensation period. The accuracy of the proposed equation was suitably indicated by the value of regression coefficient (R^2) which is defined as

$$R^2 = 1 - \frac{\sum_{i=1}^{z}(M_{\text{calculated}} - M_{\text{experiment}})^2}{\sum_{i=1}^{z}(M_{\text{experiment}})^2 - \frac{\left(\sum_{i=1}^{z} M_{\text{experiment}}\right)^2}{z-k}}, \qquad (2)$$

where z and k are the numbers of data points and parameters, respectively.

The coefficients in Eq. (1) which were correlated with the superheated-steam temperature and the bed height were as follows ($R^2 = 0.97$):

$$A = -0.00290T_{st,i}H_b + 0.00305T_{st,i} + 0.0216H_b + 0.666$$

$$k_1 = -0.00750T_{st,i}H_b + 0.00392T_{st,i} + 0.706H_b - 0.396$$

$$B = 0.00188T_{st,i}H_b - 0.00205T_{st,i} + 0.0402H_b + 0.243$$

$$k_2 = -0.0727T_{st,i}H_b + 0.0135T_{st,i} - 0.905H_b - 0.244$$

where $T_{st,i}$ is the inlet steam temperature (°C) and H_b is the bed depth (m). The experimental data and the predicted drying curve are presented in Fig. 6, showing the agreement between the experimental data and the proposed equation over the long drying period.

3.4. Head rice yield

The behaviour of the head rice yield in the superheated-steam fluidised bed dryer under different drying conditions is shown in Fig. 7. The reference head rice yield of samples was 39.95 ± 0.45% (mean ± standard errors). When the paddy was subjected to drying with steam, the results clearly show that the head rice yield from the samples can be maintained or even improved over that from the reference samples, with the values being in a wide range of 100–180% depending upon the final moisture content. At a final moisture content above 18% d.b., the relative head rice yield is rather constant, showing values between 160% and 180%. After that, the head rice yield rapidly decreases. The higher head rice yield when compared to the reference one is due to the

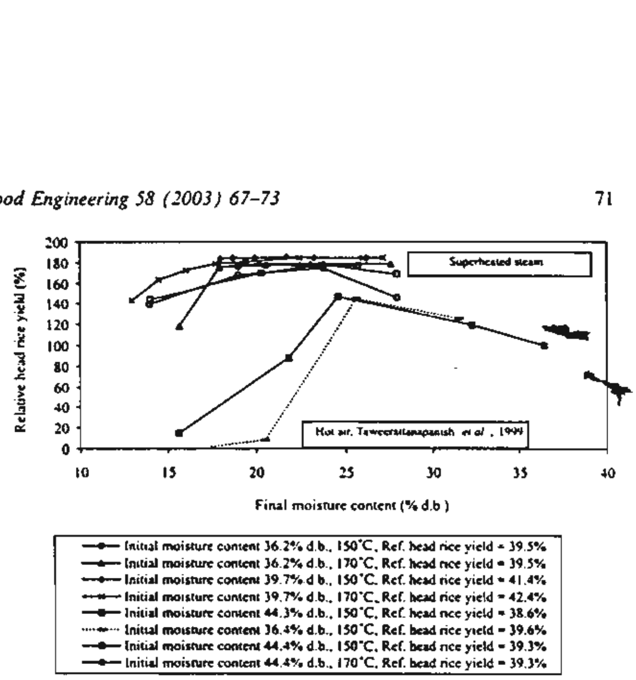

Fig. 7. Relationship between relative head rice yield and final moisture content during drying in hot air and superheated steam.

effect of partial gelatinisation occurring in the paddy grain. To confirm our explanation, we quantitatively determined that white belly occurred, as will be shown in Fig. 8. In gelatinisation steps, when high moist paddy is heated up and grain temperature reaches a temperature between 65 and 70 °C, its starch cell will swell with loss of birefringence (Atwell, Hood, Lineback, Varrino Marston, & Zobel, 1998; Zobel, 1984). This causes protein denaturation which will then penetrate into the void spaces amongst the starch granules, resulting in reduction of fissures within the grain kernels (Ranghavendra Rao & Juliano, 1970; Dimopoulos & Muller, 1972). Consequently, the paddy dried by superheated steam becomes rigid and tough, and can resist milling. That is the reason why the head rice yield of

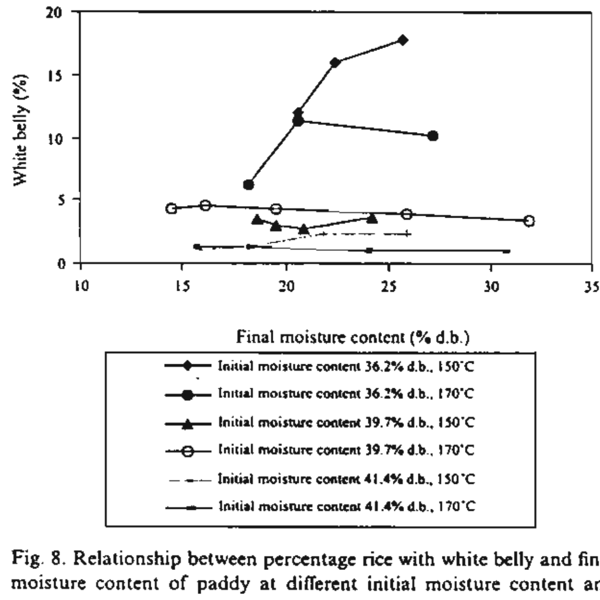

Fig. 8. Relationship between percentage rice with white belly and final moisture content of paddy at different initial moisture content and temperature.

paddy dried in the steam is higher than that of the reference method.

However, the drop in head rice after 18% d.b. may be caused by the prevalent contribution of the tension near the surface and the compression at the center of kernel, leading to fissure development although some of the fractures and void space on the grain surface disappeared in the early drying period due to swelling of starch granules.

The head rice yield of paddy obtained from superheated steam drying was compared to that obtained from hot air drying conducted by Taweerattanapanish, Soponronnarit, Wetchacama, Kongseri, and Wongpiyachon (1999). The results are shown in Fig. 7, indicating that the head rice yields of paddy samples are lower from hot air than from superheated steam. This is because the evaporation of water from the grain surface into hot air occurs close to wet-bulb temperature and the moisture removal is very fast in the initial drying period without condensation. Hence, the drying goes on with lower degrees of gelatinisation, as compared to that with superheated steam.

3.5. Rice whiteness

The change in the colour of samples from the steam temperatures of 150 and 170 °C and initial moisture contents of 36% and 44% d.b. is shown in Fig. 9. The relative rice whiteness curves in the first 3 min of drying steeply changes from the original relative value of 100% and afterwards there appears to be slight alternations with the final moisture content. Such a colour change characteristic for the steam drying has a more serious effect as compared to the hot air drying of work of Taweerattanapanish et al. (1999) as depicted in Fig. 9, showing the noticeably lower value of the relative rice

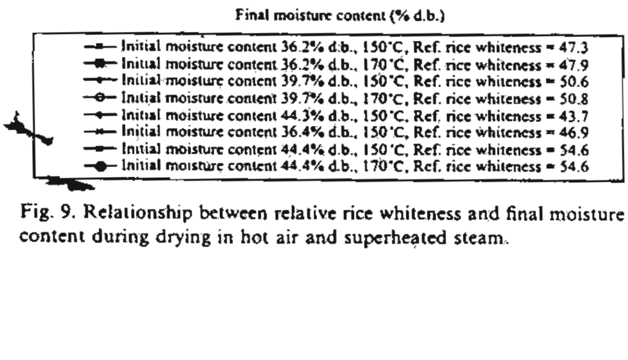

Fig. 9. Relationship between relative rice whiteness and final moisture content during drying in hot air and superheated steam.

whiteness for the steam. The main cause of the rapid change in the colour is partly due to the steam condensation onto the paddy surface. The bran covered around the kernel is dissolved and then absorbed by the endosperm. To justify the explanation, the quantity of bran was checked after milling the brown rice at a measured value of 3.4–5.2% and was found to be lower than that from the reference sample (10.2–10.8%).

The temperature used for drying is also an important factor influencing the degree of whiteness; the higher temperature causes a lower value of whiteness. The illustration of this effect can be seen in the case of moisture content 36.2% d.b. and temperatures 150 and 170 °C, showing a relative value of 55 at 150 °C and of 50 at 170 °C for the final moisture content of 23–24% d.b.

3.6. White belly

White belly in rice kernel is an indication of gelatinisation as previously explained. The individual head rice kernels after milling were graded manually to check the white belly. Kernels which have an opaque white area higher than 50% of its total area were deemed to be the white belly category, according to Thai Standard Rice (Ministry of Commerce, Thailand, 1997). The white bellies found in the experiments frequently occurred at the central area of kernel and the area near the endosperm. The percentage of white belly shown in Fig. 8 was calculated as the number of white belly kernels divided as the total number of head rice kernels. It is evident that the amount of white belly kernels depends strongly on the initial moisture contents, but it is weakly dependent on the steam temperature used. The percentage of white belly kernels is significantly lower with higher initial moisture contents. For example, the amount of white belly kernels at 150 °C is 10% for the initial moisture content of 36.3% d.b. while it is lower than 5% and 2% for the initial moisture content of 39.7%, 41.4% d.b., respectively. The lower percentage of white belly kernels may results from the higher degree of gelatinisation. In commercial practice, white belly kernels of less than 1.5% indicate premium quality parboiled rice.

From the experimental results, they indicate that when using superheated steam as drying medium, dried paddy possesses characteristics of parboiled rice. This technique can be replaced the traditional processes of making parboiled rice, which consisted of soaking, steaming and drying.

4. Conclusions

The minimum fluidising velocity for paddy in superheated steam is approximately 2.6 m/s. In the first half minute of drying paddy with superheated steam using a fluidised bed, a small amount of moisture content is gained from the steam condensation onto the surface and the gain in moisture content is independent of the steam temperature. After the rise in moisture content, the moisture content starts to decrease and can be suitably explained by a two series exponential equation, in which the parameters correlate statistically with the bed depth and the temperature, the latter being more important.

In superheated steam drying, more stable head rice yield over a wider range of final moisture contents, together with higher head rice yield, when compared to those from hot air drying, is obtained while rice whiteness apparently darkens, making it poorer quality. In addition to such qualities, the percentage of white belly kernels decreases with increase in the initial moisture content, providing relatively higher head rice yield. To maintain good head rice yield, it is recommended that high moist paddy should not be dried to lower than 18% d.b.

Acknowledgements

The authors would like to express their sincere thanks to the Thailand Research Fund for financial support, Division of Agricultural Engineering, Department of Agriculture for testing quality of milling and Pathum Thani Rice Research Center for testing the physical quality of rice.

References

AACC (1995). Approved method of the American Association of Cereal Chemist, 9th ed. St. Paul, MN: AACC.

Atwell, W. A., Hood, L. F., Lineback, D. R., Varrino Marston, E., & Zobel, H. F. (1998). The terminology and methodology associated and basic starch phenomena. *Cereal Foods World, 33*, 306–308, 310–311.

Dimopoulos, J. S., & Muller, H. G. (1972). Effect of processing conditions on protein extraction and composition and on some other physicochemical characteristics of parboiled rice. *Cereal Chemistry, 49*, 54–62.

Ergun, S. (1952). A basic of fluidisation. *Chemical Engineering Progress, 48*, 89–93.

Geankoplis, C. J. (1995). *Transport processes and unit operations* (third ed., p. 118). Singapore: Prentice Hall.

Ministry of Commerce, Thailand (1997). Thai Standard Rice, http:// 203.151.17.19/document/grain/english/standard.htm, last revised on 20 June 2002.

Prachayawarakorn, S., Soponronnarit, S., & Jaisut, D. (2002). Desorption isotherms and drying characteristics of shrimp in superheated steam and hot air. *Drying Technology, 20*(3), 669–684.

Ranghavendra Rao, S. N., & Juliano, B. O. (1970). Effect of parboiling on some physicochemical properties of rice. *Journal Agricultural Food Chemistry, 18*, 289–294.

Soponronnarit, S., & Prachayawarakorn, S. (1994). Optimum strategy for fluidised bed paddy drying. *Drying Technology, 12*(7), 1667–1686.

Sutherland, J. W., & Ghaly, T. F., (1990). Rapid fluid-bed drying of paddy rice in the humid tropics, Presented Thirteenth ASEAN Seminar on Grain Postharvest Technology, Bandar Seri Begawan, Brunei Darussalam, p. 1–12.

Tang, Z., & Cenkowski, S. (2000). Dehydration dynamics of potatoes in superheated steam and hot air. *Canadian Agricultural Engineering, 42*(1), 6.1–6.13.

Taweerattanapanish, A., Soponronnarit, S., Wetchacama, S., Kongseri, N., & Wongpiyachon, S. (1999). Effect of drying on rice yield using fluidisation technique. *Drying Technology, 17*(1 and 2), 345–353.

Yoshida, T., & Hyodo, T. (1963). Evaporation of water in air, humid air and superheated steam. *Industrial and Engineering Chemistry Process Design and Development, 9*(2), 207–214.

Zobel, H. F. (1984). Gelatinization of starch and mechanical properties of starch pastes. In R. L. Whistler, J. N. Bemiller, & E. F. Paschall (Eds.), *Starch: chemistry and technology* (second ed., pp. 285–309). London: Academic Press.

ELSEVIER

Journal of Food Engineering 59 (2003) 369–377

JOURNAL OF FOOD ENGINEERING

www.elsevier.com/locate/jfoodeng

Optimization of heat pump fruit dryers

U. Teeboonma *, J. Tiansuwan, S. Soponronnarit

School of Energy and Materials, King Mongkut's University of Technology, Thonburi, Suksawat 48 Rd., Thunkaru, Bangkok 10140, Thailand

Received 25 July 2002; accepted 1 December 2002

Abstract

The most important factors when examining the optimum conditions of heat pump fruit dryers (HPD) and for minimizing HPD cost are recycle air ratio, evaporator bypass air ratio (BP), airflow rates, and drying air temperature. Mathematical models of papaya and mango glacé drying using HPD are developed and validated experimentally. The optimum criterion is minimum annual total cost per unit of evaporating-water. The effects of initial moisture content, cubic size, and effective diffusion coefficient of products on the optimum conditions of HPD are also investigated. The results showed that the optimum conditions of both products are not similar, especially for the optimum airflow rate and evaporator BP. For sensitivity analysis, the annual total cost per unit of evaporating-water in a HPD is linearly proportional to both interest rate and electricity price, and decreased with increasing life-time. Finally, physical properties of the product significantly affect the optimum airflow rate and evaporator bypass air ratio.

Keywords: Heat pump drying; Mathematical models; Physical properties

1. Introduction

Conventional hot air dryers are widely used for fruit drying. However, the high drying temperature usually causes low quality of products. Heat pump dryers are an alternative method for drying products with lower energy consumption, less relative humidity, and lower temperature (Vázquez, Chenlo, Moreria, & Cruz, 1997). Preliminary studies found that the color and aroma qualities of dried agricultural products using heat pumps were better than those products using conventional hot air dryers (Prasertsan & Saen-saby, 1998; Soponronnarit, Nathakaranakule, Wetchacama, Swasdisevi, & Rukprang, 1998; Strommen, 1994). To maximize specific moisture extraction rates, Clement, Jai, and Jolly (1993) recommended that evaporator bypass air ratio (BP) should be around 60–70%. To minimize energy consumption, Soponronnarit et al. (1998) suggested that evaporator BP should be around 86–90%. Achariyaviriya, Soponronnarit, and Terdyothin (2000a) had developed an empirical model of heat pump dryers and recommended that the best conditions giving maximum specific moisture extraction rates were the airflow rate of 10.3 kg/h kg of dry papaya, evaporator BP of 85%, recycle air ratio (RC) of 100%, and drying air temperature of 56 °C. When studying the economics of using heat pumps, electrical heaters, and fuel burners to dry grain, Meyer and Greyvenstein (1992) recommended that the heat pump dryer was more economical than other systems although the initial cost was higher. A similar suggestion was made by Prasertsan and Saensaby's work (1998).

The objectives of this research were to determine the optimum conditions of heat pump fruit dryers to minimize annual total cost per unit of evaporating-water of HPD, and to investigate the effects of physical properties of products on the optimum conditions. Mathematical models of papaya and mango glacé drying using heat pump dryers were developed, validated, and implemented in this optimization program.

2. Materials and methods

2.1. Development of mathematical model

The schematic diagram of a heat pump fruit dryer is illustrated in Fig. 1. The air flows through the drying chamber and picks up the moisture of the product.

* Corresponding author.
E-mail address: umphisak@hotmail.com (U. Teeboonma).

0260-8774/03/$ - see front matter © 2003 Elsevier Science Ltd. All rights reserved.
doi:10.1016/S0260-8774(02)00496-X